geologica acta

Citation: Salas, R., Guimerà, J., Bover-Arnal, T., Nebot, M., 2026. Structuration and sedimentary response to continental Mesozoic rifting in northeastern Iberia. Geologica Acta, 24.9, 1-29. DOI: 10.1344/GeologicaActa2026.24.9

Online ISSN: 1696-5728

Structuration and sedimentary response to continental Mesozoic rifting in northeastern Iberia

Ramon Salas[1,3,4] Joan Guimerà[2,3] Telm Bover-Arnal[1,3] Marina Nebot[2]

[1]Departament de Mineralogia, Petrologia i Geologia Aplicada, Facultat de Ciències de la Terra, Universitat de Barcelona
Carrer Martí i Franquès s/n, 08028 Barcelona, Catalonia, Spain. Salas E-mail: ramonsalas@ub.edu
Bover-Arnal E-mail: telm.boverarnal@ub.edu

[2]Departament de Dinàmica de la Terra i de l'Oceà
Facultat de Ciències de la Terra, Universitat de Barcelona, Carrer Martí i Franquès s/n, 08028 Barcelona, Catalonia, Spain.
Guimerà E-mail: joan.guimera@ub.edu Nebot E-mail: marinanebotmiralles@gmail.com

[3]Institut de Recerca GEOMODELS
Carrer Martí Franquès s/n, 08028 Barcelona, Catalonia, Spain.

[4]Royal European Academy of Doctors
Via Laietana 32-3, 08003 Barcelona, Catalonia, Spain.

ABSTRACT

Iberia and its oceanic margins provide evidence of a large rift system developed in three phases: i) late Permian–Middle Triassic, ii) Late Jurassic, and iii) Barremian–early Albian. These rifting events were coeval with the opening of the Alpine Tethys, the North-Atlantic, and the Bay of Biscay domains, respectiely. The three Mesozoic rifting phases controlled the development of Iberian intraplate rift basins, including the Maestrat and Garraf basins, which are the focus of this study. Each of these rifting stages was followed by a period of decelerated or post-rift thermal subsidence. The first post-rift phase, spanning the Late Triassic to the early Late Jurassic, was interrupted by a short-lived interval of rapid syn-rift subsidence during the Hettangian, here referred to as the Hettangian event. Rifting cycles 2 and 3 are separated by the Neocomian event, which corresponds to an interval of decelerated subsidence. The earliest rifting phase is associated with an early inception of saline tectonics in the Maestrat Basin, and was accompanied by magmatism and took place in an arid climate setting, whereas the second and third rifting stages were essentially amagmatic and occurred under humid (sub)tropical conditions. The structural style during polyphase rifting is characterized by extensional systems involving the uppermost part of the crust, with basal faults located at a depth of 7 to 10km. The Maestrat and Garraf basins developed during the Barremian–early Albian period were bounded by decakilometric normal faults with kilometric dip-slip, and were later inverted during the Paleogene contraction, giving rise to the fold-and-thrust systems of the Iberian and Catalan Coastal chains. Vertical movements, uplift and fault-induced subsidence, and the prevailing climate conditions were the two principal controls on the sedimentary record of the Iberian intraplate rift basins.

KEYWORDS **Iberia, Rifting, Mesozoic, Iberian Chain, Catalan Coastal Chain.**

INTRODUCTION

Rift systems represent the lithosphere response to stretching, characterized by the growth and linkage of normal faults (Miall, 2010). In eastern Iberia, the predominant Mesozoic extensional structure was the half-graben (Nebot and Guimerà, 2016a, b). In addition to vertical movements of uplift and subsidence, as well as the interaction and linkage of normal faults through the creation and migration of grabens and relay zones, the main general factors controlling rift basin stratigraphy include eustatic sea-level changes and sediment supply, both of which are strongly influenced by climate (Gawthorpe and Leeder, 2000).

During the break-up of Pangea, which led to the opening of the Western Tethys and the North Atlantic, Iberia was repeatedly affected by extensional tectonics. One of these Mesozoic rifts, trending NW-SE across Iberia, is the Iberian Rift System (Salas *et al.*, 2001). Rifting and wrench activity in Iberia persisted intermittently until Late Jurassic and mid-Cretaceous times, when Iberia separated from Europe in conjunction with the opening of the oceanic Bay of Biscay Basin.

Depending on the position within the rift, fault activity intensified during the Early–Middle Triassic, Kimmeridgian, and Barremian, leading to the formation of basin depocenters. This increased the shoreline slope towards deeper water and caused pulses of relative sea-level change. The resulting sedimentary record includes continental to marine, mixed carbonate-siliciclastic deposits. Among the documented rifting cycles, the Barremian–Aptian phase is the least affected by erosion, thereby allowing for a more comprehensive characterization of its extensional system.

This paper addresses the sedimentary and structural evolution of the Mesozoic Iberian Rift System, also referred to as the Iberian Basin, which currently corresponds to the Iberian and Catalan Coastal chains, a system of intraplate fold-and-thrust belts. More precisely this paper focuses on the Maestrat Basin located in the eastern part of the Iberian Chain and the Garraf Basin situated in the Catalan Coastal Chain (Fig. 1).

The specific objectives of the study are: (i) to characterize the stratigraphy and main unconformities of the study area; (ii) to describe the rift and post-rift evolution of the basins by field and subsidence techniques; (iii) to study the geometry and evolution of the Mesozoic and Cenozoic structures by integration of available subsurface data, including 2D seismic profiles and exploration wells, and new field data; and (iv) to evaluate the depositional and structural controls on the process affecting the intraplate rift basins and their evolution. The results can be used to establish predictive relationships for the improved characterization of intraplate rift basins at seismic-scale, even when subsurface data are limited.

GEOLOGICAL CONTEXT

The study area is located in the E-W-trending, N-verging Linking Zone between the NW-SE-trending Iberian Chain and the NE-SW-trending Catalan Coastal Chain (Guimerà, 1983, 1984, 2018) (Fig. 1A). These chains are the result of the Cenozoic inversion of the Late Jurassic–Early Cretaceous Maestrat and Garraf basins, which were one of the most subsident basins of the southern Mesozoic Iberian Rift System (Anadón *et al.*, 1979; Guimerà, 1988; Salas *et al.*, 2001).

Previous studies have described the Iberian Rift System as having developed during the Mesozoic and undergoing two major rifting phases: in the late Permian–Triassic, and the Late Jurassic–Early Cretaceous, each followed by periods of reduced extensional activity during the Early–Middle Jurassic and the middle Albian–Maastrichtian (Salas and Casas, 1993; Salas *et al.*, 2001). More recently, Salas *et al.* in Martín-Chivelet *et al.* (2019) refined the interpretation of the Iberian Rift System's evolution, proposing a more detailed model consisting of six distinct syn-rift and post-rift phases: (i) late Permian–Triassic rifting, (ii) Early and Middle Jurassic post-rift, (iii) Late Jurassic rifting, (iv) Neocomian (late Berriasian–Hauterivian) post-rift, (v) Early Cretaceous (Barremian–early Albian) rifting, and (vi) Late Cretaceous post-rift.

The earliest rifting phase was accompanied by magmatism and developed under arid climate conditions, whereas the second and third rifting stages were essentially amagmatic and occurred in a humid subtropical climate zone. The second rifting cycle commenced in the Kimmeridgian and was associated with intense rifting activity in the North Atlantic domain, including the Lusitanian Basin (Pimentel and Pena dos Reis, 2016). According to Salas *et al.* in Martín-Chivelet *et al.* (2019), this rifting cycle (Kimmeridgian–early Berriasian) was followed by a stage of relative tectonic quiescence of decelerated post-rift thermal subsidence during the Neocomian (late Berriasian–Hauterivian), characterized by the deposition of the Purbeck facies.

Rifting resumed during the Barremian and persisted until the early Albian. Intraplate extension reached its peak during this cycle, in marked contrast to the limited coeval extension recorded along the Atlantic margin, which underwent thermal subsidence at that time (Pimentel and Pena dos Reis, 2016; Stampfli, 2000). The initial sedimentary record grades from restricted marine

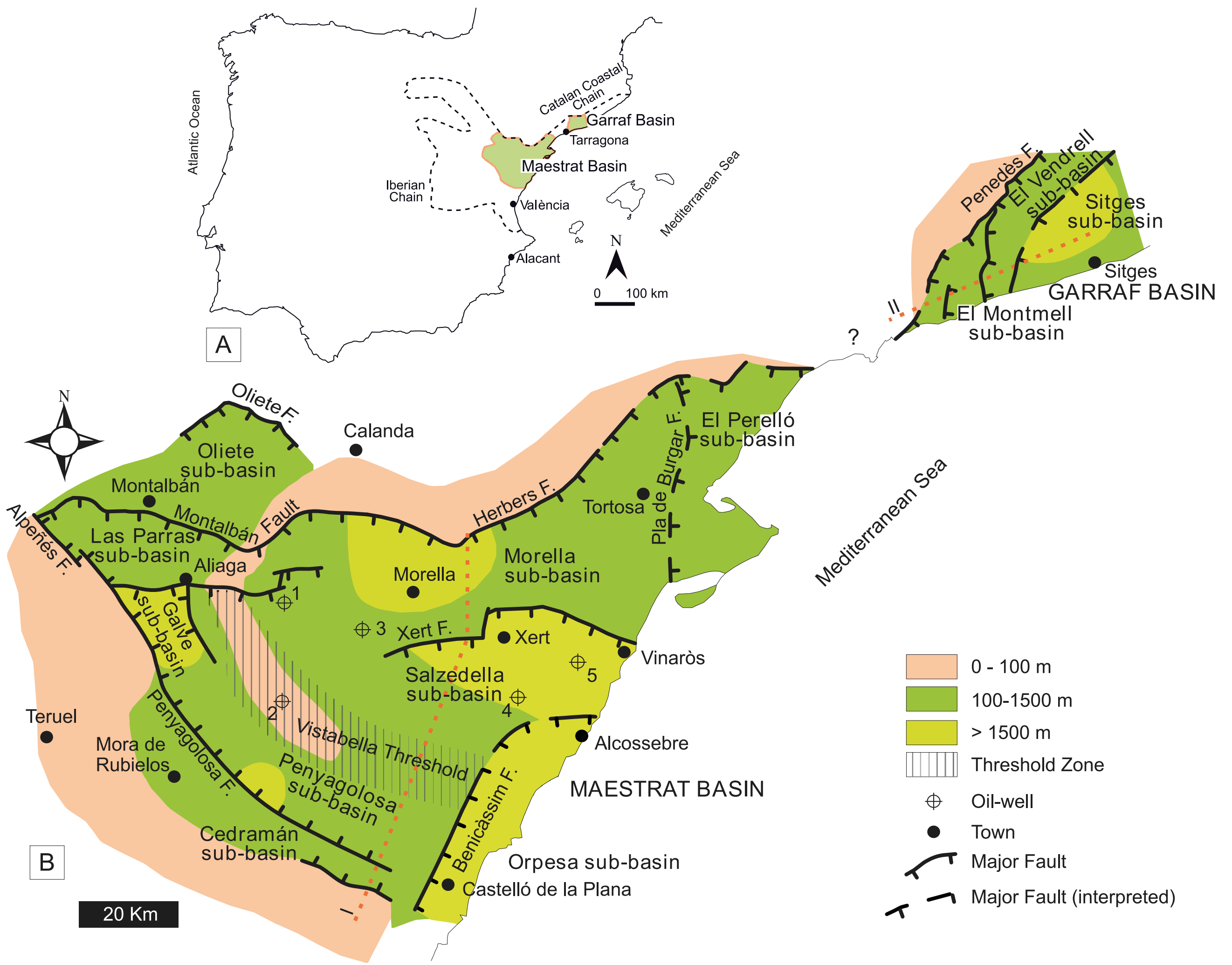

FIGURE 1. A) Location of the Maestrat and Garraf basins within the Iberian Peninsula. B) Simplified structural map of the Maestrat and Garraf basins during Late Jurassic Rifting Cycle 2, the Neocomian event (late Berriasian–Hauterivian) and Early Cretaceous (Barremian–early Albian) Rifting Cycle 3. Note that this Late Jurassic–Early Cretaceous complex cycle of rifting (*sensu* Salas *et al.*, 2001) structured the basins into several main fault zones and sub-basins. Inset: the location of the cross-sections I and II shown in Fig. 2. Oil-wells: 1= Mirambell-1, 2= Maestrazgo-2, 3= Bovalar-1 and Bovalar-2, 4= Salzedella-1, 5= Maestrazgo-1. Modified from Salas *et al.* in Martín-Chivelet *et al.* (2019).

to lacustrine and alluvial deposits, with accumulations of freshwater carbonates and siliciclastics deposited in embayment settings, characteristic of the Weald facies (*e.g.*, Caja Rodríguez, 2004).

During the Aptian, fault activity generated several depocenters throughout the rift system and led to significant changes in accommodation. The resulting sedimentary record includes progradational fluvio-deltaic sands, basinal marls, and carbonate platforms, among which the rudist-dominated Urgonian facies association is particularly characteristic (*e.g.*, Bover-Arnal *et al.*, 2010; Salas, 1987; Vennin and Aurell, 2001).

The progressive cessation of continental rifting during the Albian was coeval with the formation of rapidly subsiding depocentres in the marginal areas of the basins, accompanied by increased sediment fluxes in fluvial and deltaic systems (*i.e.*, Escucha Formation; Querol *et al.*, 1992). The intra-Albian regional unconformity at the base of the fluvio-deltaic Utrillas Formation marks the onset of the post-rift thermal subsidence stage during the middle Albian (*e.g.*, Salas and Casas, 1993).

The second and third cycles of accelerated subsidence were considered by Salas *et al.* (2001) as a single, complex rifting cycle spanning from the Late Jurassic to the early Albian. This interval was characterized as displaying two main pulses of rapid subsidence, occurring in the Late Jurassic and Early Cretaceous, separated by a stage of decelerated subsidence throughout the Neocomian.

During the second and third rifting cycles, rift-related structures were aligned into two main branches: the Pyrenean Rift and the Iberian-Catalan Rift. Both diverged from the Bay of Biscay and were bordered by the uplifted Hesperian and Ebro hinterland areas, which acted as persistent source areas for siliciclastic supply. The dominant direction of sedimentary influx was from west to east (Salas *et al.*, 2010). Notably, the Columbrets Basin (València Trough) underwent extreme Mesozoic crustal thinning during these rifting cycles (Etheve *et al.*, 2018; Fang *et al.*, 2021; Ramos *et al.*, 2023; Roca, 1996; Roma *et al.*, 2018).

The Upper Jurassic–Lower Cretaceous Maestrat and Garraf basins were bounded by decakilometric extensional faults with kilometric normal displacement (Figs. 1B, 2). Many of these faults underwent contractional reactivation during the Cenozoic (Baqués *et al.*, 2012; Nebot and Guimerà 2016a, b; Salas *et al.*, 2001), and were later covered by Neogene sediments (Fig. 3). As a result, the precise location of some bounding faults, particularly those linking the Maestrat and Garraf basins, remain uncertain.

The Maestrat Basin was generated by a system of extensional faults of listric geometry, as is deduced from the depocenters attached to the fault and rocks thinning away from it (Fig. 2). Its northern boundary is composed of a roughly E-W-trending, south-dipping fault set, with the Montalbán and Herbers faults being the major ones. The southern boundary is defined by NW-SE-trending, northeast-dipping faults, primarily the Penyagolosa and Alpeñés faults (Figs. 1B, 2, 3). Due to their listric nature, these faults generated wide rollover structures developed in their hanging-walls, with depocentres positioned adjacent to the fault traces. Moreover, the interaction between the rollovers related to the northern and southwestern fault boundaries generated a zone of reduced subsidence between them, known as the Vistabella Threshold (Figs. 1B, 2; Salas and Guimerà, 1996). Additional extensional faults are present between the main bounding structures, predominantly E-W-trending (Xert and Aliaga faults), with some oriented NE-SW, such as the Benicàssim Fault (Figs. 1B, 3). These internal structures contributed to the compartmentalization of the Maestrat Basin into several sub-basins: Las Parras, Galve, Oliete, Penyagolosa, Cedramán, Orpesa, La Salzadella, El Perelló, and Morella (Figs. 1B, 2; Salas *et al.* in Martín-Chivelet *et al.*, 2019 ; Salas and Guimerà, 1996). The Oliete and Cedramán sub-basins are located in a marginal position relative to the major faults, lying to the north and south respectively.

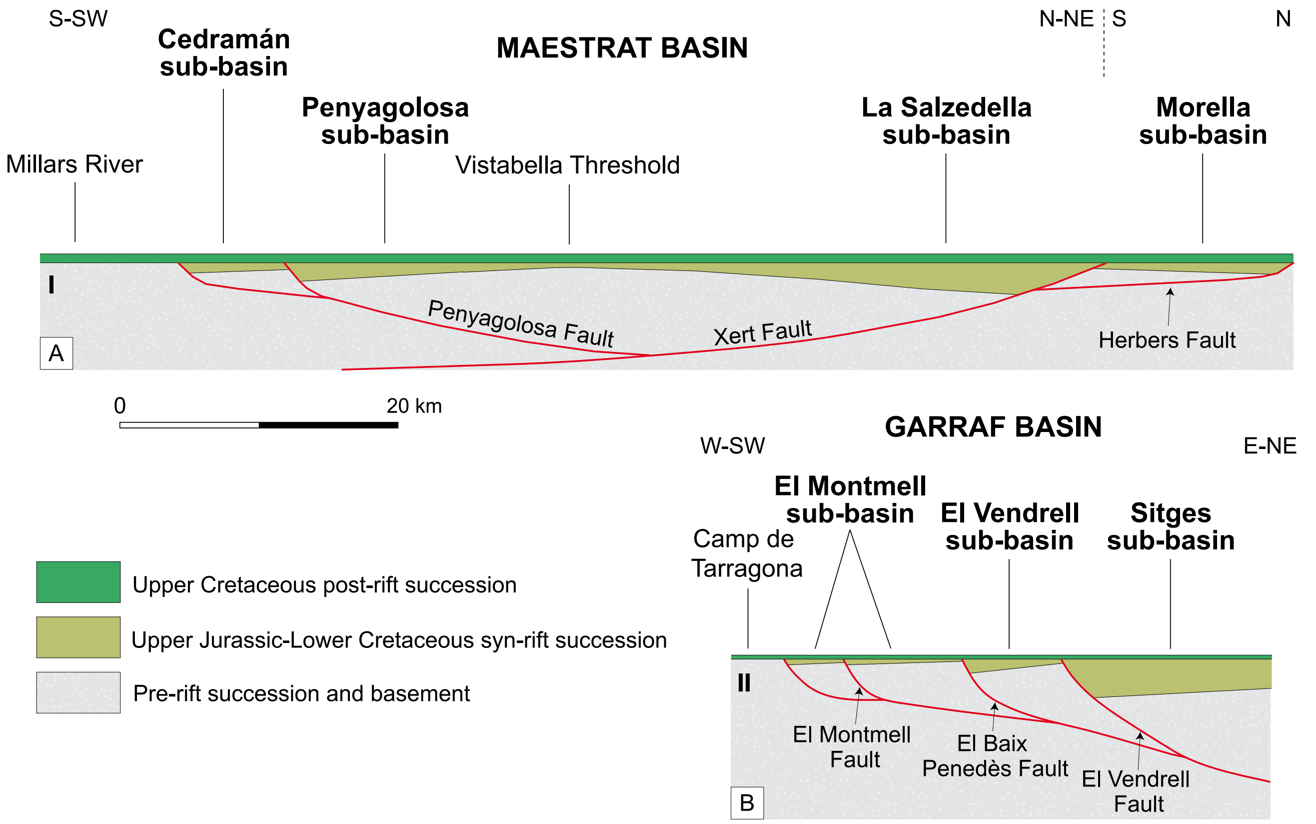

FIGURE 2. A) and B) Schematic cross-sections of the Maestrat and Garraf basins, respectively, traversing main depocenters and structures. See Fig. 1 for locations. Modified from Salas *et al.* in Martín-Chivelet *et al.* (2019).

The Garraf Basin is bounded to the northwest by the NE-SW-trending Penedès Fault (Anadón *et al.*, 1979), likely a continuation of the Herbers Fault (Fig. 1B). Several faults with a listric geometry subdivide the basin into three sub-basins, the largest of which is the Sitges Sub-basin (Figs. 1A, 2).

Considering the areal extension of the faults and the amount of normal displacement required to generate the sedimentary thickness recognized in both the Maestrat and Garraf basins, the extensional system responsible for their formation must have involved the Variscan basement. An extensional system rooted in the upper crust (at depths of 7-10km) is therefore proposed. This system coincides with that inferred for the Cenozoic contractional regime, which inverted the Iberian Basin Rift System (Guimerà and Álvaro, 1990; Seillé *et al.*, 2015).

The Iberian intraplate rift basins, such as the Maestrat and Garraf basins, were inverted during the Paleogene contraction during the Alpine Orogeny, leading to the formation of the Iberian and Catalan Coastal fold-and-thrust belts (Nebot and Guimerà, 2016a, b; Salas *et al.*, 2001). Subsequently, late Neogene extension related to the opening of the Mediterranean overprinted these structures, defining the present-day configuration of the region (Guimerà, 1988).

MATERIALS AND METHODS

The conceptual model of the formation and evolution of the Mesozoic Iberian Rift System and its Cenozoic inversion is the result of 40 years of fieldwork, laboratory analysis, and desk-based research. Over this period, 28 stratigraphic sections were measured, totaling more than 19km of logged strata, and correlated across the study area to: (i) identify key lithofacies variations and their stratal relationships, (ii) observe and identify fossil content and changes in sedimentary facies, and (iii) characterize stacking patterns and stratal terminations.

The burial history of the Maestrat and Garraf basins was assessed by subsidence analysis, using conventional

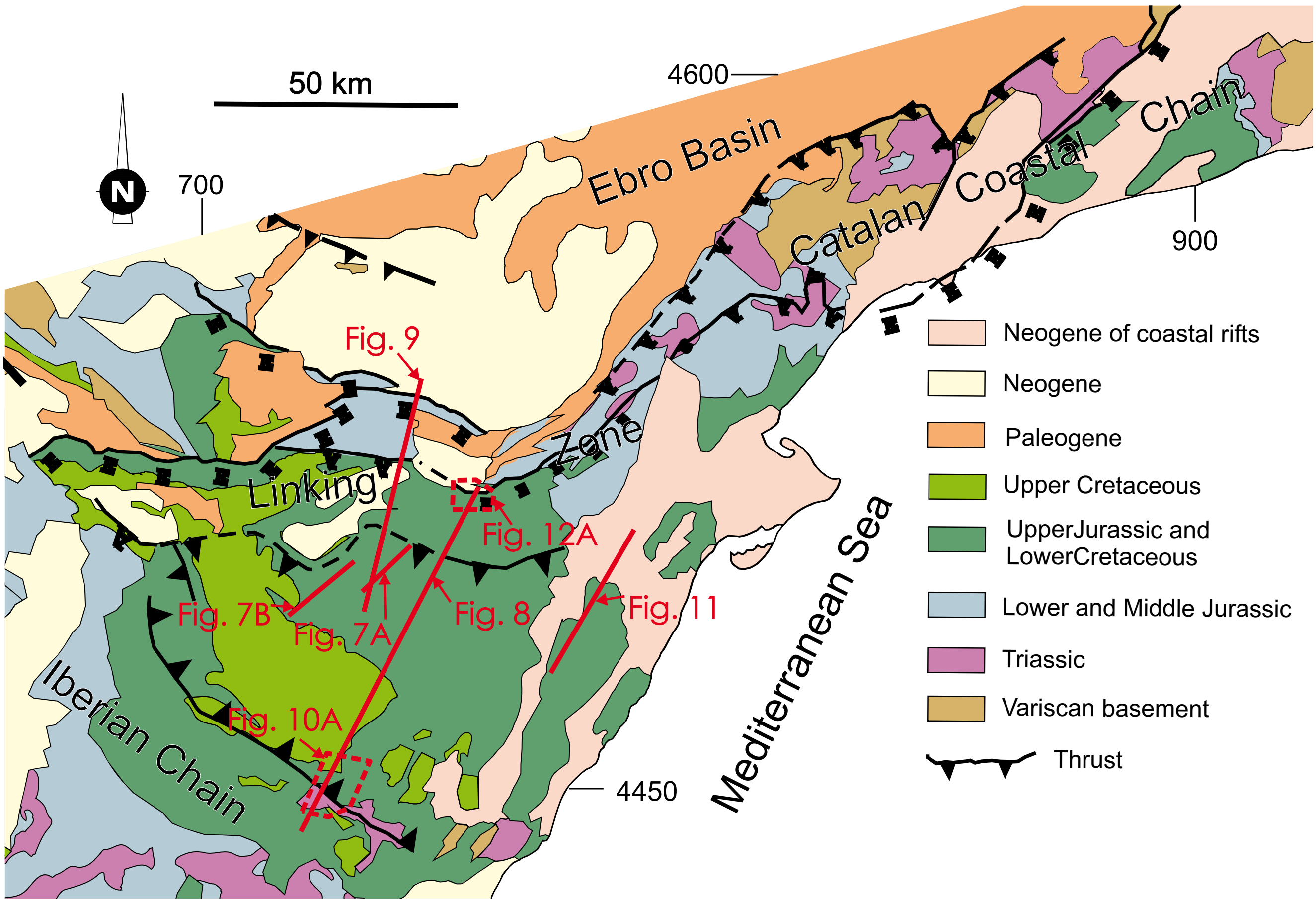

FIGURE 3. Simplified geological map of the Maestrat and Garraf basins and surrounding areas, showing the location of the cross-sections illustrated in figures 7-12.

back-stripping methodologies (Bond and Kominz, 1984; Sclater and Christie, 1980; Steckler and Watts, 1978; Watts, 1981). Decompacted subsidence curves were calculated using an Excel macro created by D. Waltham (Royal Holloway, University of London), following the methodology outlined by Allen and Allen (1990), and calibrated to the time scale of Cohen *et al.* (2025) and Gale *et al.* (2020) . Input parameters included lithology, unit age, present-day depth, estimated paleobathymetry, and eustatic sea-level at the time of deposition. Decompaction was carried out using porosity-depth relationships and lithology-specific density values, while paleobathymetry estimates were derived from the interpreted depositional environments. Subsurface data from the Maestrazgo-1, Salzedella-1, and Mirambell-1 wells (Fig. 1B; Lanaja, 1987; Martínez-Abad, 1991) were integrated with field observations and stratigraphic data from outcropping sections in the Garraf Basin to account for the effects of post-Eocene erosion linked to the Alpine contractional uplift. This combined dataset enabled a more accurate reconstruction of original sediment thicknesses and provided key constraints for backstripping analysis. The total thicknesses of the Mesozoic successions modeled are: 5339m in Maestrazgo-1, 3188m in Mirambell-1, and 3432m in Garraf. The timing of rift and post-rift phases is based on Salas *et al.* (2001) and Salas *et al.* in Martín-Chivelet *et al.* (2019). To calculate tectonic (unloaded) subsidence, we applied the McKenzie (1978) stretching model for intracontinental rift basin formation, assuming local isostatic equilibrium.

To characterize the structure of the area studied, geologic mapping at several scales was performed, including several thousand strike-and-dip data of bedding and faults. Cross-section construction was based on the kink method, and its restoration to the end of Mesozoic was performed preserving line-length and surface. The geometry of the basement fault was reconstructed using the Move® software. Seismic profiles and exploration wells available were also considered.

RESULTS

Stratigraphy

A comprehensive and updated chronostratigraphic framework is proposed for the Maestrat and Garraf basins (Fig. 4), grounded in the geological evidence presented in this subsection and integrating new observations and data obtained since Salas *et al.* (2001). The Mesozoic materials in the study area, including both the rocks filling the Upper Jurassic–Lower Cretaceous Maestrat and Garraf basins and those in their substratum, and the overlying Cenozoic sedimentary cover, are subdivided into four major sequences bounded by regional unconformities (D1-D5) of upper Permian–Triassic, Jurassic, Lower Cretaceous, and Upper Cretaceous age (Fig. 4). These sequences were deposited during different rifting and post-rifting events within the Iberian Rift System (Salas and Casas, 1993; Salas *et al.* in Martín-Chivelet *et al.*, 2019; Salas *et al.*, 2001).

The regional unconformity D1 corresponds to the Variscan unconformity, whereas D3 represents a syn-rift unconformity at the termination of rifting cycle 2. Similarly, D4 corresponds to post-rift unconformity associated with the end of rifting cycle 3. Both D3 and D4 are characterized by distinct angular geometries. In contrast, D2 represents a different case. While it has previously been interpreted as a post-rift unconformity (Salas *et al.*, 2001), this study interprets D2 as an erosional surface that marks the onset of a short-lived episode of accelerated subsidence during the deposition of Hettangian breccias, within a longer-term post-rift phase spanning from the Late Triassic to the Oxfordian (Fig. 4). Therefore, D2 would not represent a post-rift unconformity, but rather an erosional surface associated with renewed tectonic activity during the latest Triassic–earliest Jurassic, herein referred to as the Hettangian rifting event. The Garraf Basin contains a discontinuous Mesozoic record, with significant gaps, particularly in the late Lias, Dogger, and late Neocomian intervals (Fig. 4).

Subsidence analysis

To evaluate the tectonic evolution of the Maestrat and Garraf basins (Fig. 1), two previously published quantitative subsidence curves from petroleum exploration wells (Salas and Casas, 1992, 1993; Salas *et al.*, 2001) were reviewed, and a new subsidence curve was calculated for the Garraf Basin (Fig. 5). Although the three resulting tectonic subsidence curves display a generally similar pattern, noticeable differences exist in both their shapes and the magnitude of tectonic subsidence. These differences primarily reflect the varying locations of the data points within the basins and the associated variations in sedimentary thickness. Nevertheless, all the curves show three distinct phases of tectonic subsidence, each characterized by an initial interval of rapid subsidence followed by a phase of decelerating subsidence. This pattern is usually diagnostic of rifting processes, which comprise an initial period of fault-controlled, rapid syn-rift subsidence, followed by a post-rift phase marked by asymptotically decreasing subsidence driven by the thermal relaxation of the lithosphere (McKenzie, 1978). Based on the interpreted subsidence phases, as well as the structural and regional context of the control points, three intervals of rapid-to-decelerated subsidence can be distinguished: 1) late Permian–Oxfordian, 2) Kimmeridgian–Hauterivian, and 3) Barremian–Maastrichtian (Fig. 5).

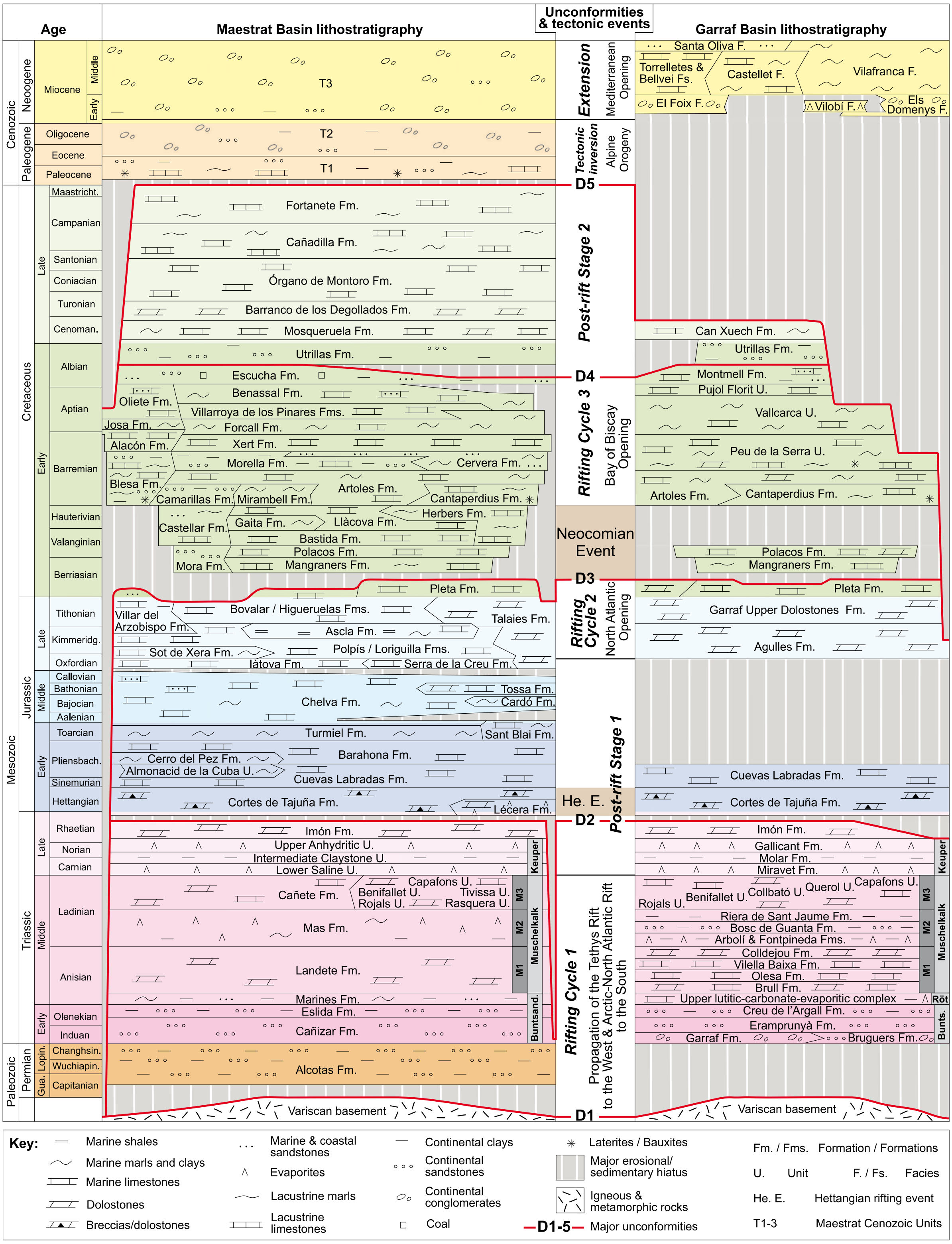

FIGURE 4. Lithostratigraphic chart of the Mesozoic Maestrat and Garraf basins and overlying Cenozoic lithostratigraphic units of the Ebro and Penedès basins. Inset: the major unconformities and tectonic events of late Paleozoic to Cenozoic age. Note that the base of the middle Albian may unconformably overlie strata ranging from the Paleozoic (including metamorphic and igneous rocks) to the Aptian. This complexity is not illustrated in the figure in order to maintain clarity and highlight main depositional trends. Based on Albrich et al. (2006), Aurell et al. (2002, 2009, 2016, 2018), Bover-Arnal et al. (2016, 2025), Campos-Soto et al. (2017), Canérot (1974), Canérot et al. (1982), Coromines (1997), Garcia et al. (2014), García et al. (2004), García-Penas et al. (2024), Giner (1980), Gómez and Goy (2004), Goy et al. (1976), López-Gómez and Arche (1992), Martín-Closas et al. (2017), Martín-Martín et al. (2005), Mas et al. (2004), Moreno-Bedmar et al. (2016, 2017), Nebot and Guimerà (2016a, b), Ortí et al. (2017), Permanyer (1990), Roca et al. (1994), Salas (1987), Salas and Casas (1993), Salas et al. (1995, 2001), Sánchez-Moya et al. (2004a, b).

During the late Permian–Oxfordian phase of tectonic subsidence, the subsidence curves display a late Permian–Middle Triassic period of rapid subsidence that decelerates during the Late Triassic–early Late Jurassic. This trend reflects the initial Rifting Cycle 1, followed by a Post-rift Stage 1, which begins with the deposition of the Keuper facies (Fig. 4). Post-rift Stage 1 includes a brief episode of accelerated subsidence during the Hettangian, particularly evident in the subsidence curve of the Mirambell-1 well (Fig. 5). This interval of rapid syn-rift subsidence, occurring within a broader post-rift phase, is interpreted as a distinct Hettangian rifting event, recorded by the deposition of the breccias of the Cortes de Tajuña Formation (Fig. 4).

The next phase of tectonic subsidence corresponds to the Kimmeridgian–Hauterivian interval. This rifting phase can be subdivided into two stages: an initial phase of rapid subsidence during the Kimmeridgian to early Berriasian (Rifting Cycle 2), followed by a phase of decelerating subsidence throughout the Neocomian (Post-rift Stage 2). The final phase of tectonic subsidence spans the Barremian–Maastrichtian. This period is marked by rapid subsidence until the early Albian (Rifting Cycle 3), coinciding with the deposition of the Escucha and Montmell formations (Fig. 4). The latter part of this rifting cycle was again characterized by decelerating subsidence rates during the middle Albian to Maastrichtian interval (Post-rift Stage 3). The intra-Albian regional unconformity, located at the base of the fluvio-deltaic Utrillas Formation (D4), marks the onset of the Late Cretaceous post-rift thermal subsidence stage, beginning in the middle Albian.

The three main rift–post-rift phases identified in the Maestrat and Garraf basins closely align with those documented in other published quantitative subsidence curves from the Iberian Basin (Arche *et al.*, 2004; Salas and Casas, 1993; Salas *et al.*, 2001; Stampfli, 2000; Van Wees *et al.*, 1998; Van Wees and Stephenson, 1995).

Structural rift framework.

The three major rifting periods (late Permian–Middle Triassic, Late Jurassic, and Barremian–early Albian) are structurally different, each controlled by an independent fault system without reactivation of earlier basin-bounding structures. A well delimited Maestrat Basin can only be clearly identified during the Barremian–Aptian period. The main structural characteristics of the three rifting phases, the intervening post-rift periods, and the Neocomian event of subsidence deceleration are described below.

Late Permian–Middle Triassic rift configuration

Triassic rocks crop out in limited areas along the northern and southern margins of the Maestrat Basin (Fig. 3). The Triassic structural and stratigraphic architecture is primarily interpreted from seismic profiles and borehole data. Upper Permian red beds and the Triassic Buntsandstein facies unconformably overlie the Variscan basement. The Muschelkalk facies are subdivided into lower and upper carbonate units, separated by a middle unit composed of halite and anhydrite interbedded with lutites. The Keuper facies exhibit a similar composition, dominated by halite and anhydrite with lutite intercalations. Overlying the Keuper succession is the uppermost Triassic carbonate-rich Imón Formation (Fig. 4).

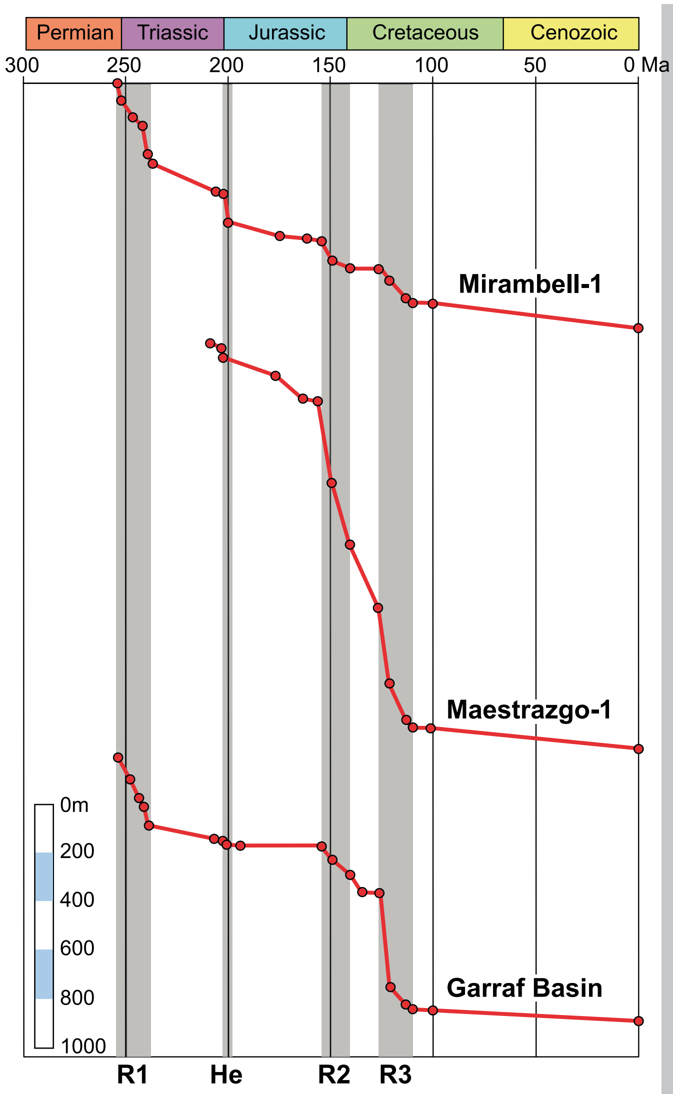

FIGURE 5. Backstripped tectonic subsidence for the Maestrat (Mirambell-1 and Maestrazgo-1 wells) and Garraf basins. Additional information was obtained from outcropping stratigraphic sections, considering the effects of Cenozoic erosion. Shaded areas indicate the three cycles of Mesozoic syn-rift subsidence and the Hettangian rifting event (He). R1=late Permian–Middle Triassic Rifting Cycle 1; R2=Kimmeridgian–early Berriasian Rifting Cycle 2; R3=Barremian–early Albian Rifting Cycle 3.

Correlation of the available petroleum borehole data reveals two distinct stratigraphic domains, interpreted to be separated by a NNE-SSW-trending normal fault (Fig. 6). Northwest of this fault, the upper Permian–Triassic stratigraphic succession is preserved with a total thickness of at least 1450m. Southeast of the fault, a reduced succession, comprising only the Buntsandstein and the post-rift Keuper facies, is observed in the Salzadella-1 and Maestrazgo-1 boreholes, with total thicknesses of 220m and 370m, respectively. Northeast of the city of Castelló de la Plana (Fig. 6), a 90m-thick carbonate-rich Muschelkalk interval overlies 300m of Buntsandstein facies (López Gómez *et al.*, 2005).

Figure 7 displays two cross-sections through the interior of the basin (refer to Fig. 3 for location). The acoustic basement, including the lower Muschelkalk, the Buntsandstein facies, and the Paleozoic, is cut by high-angle normal faults oriented NW-SE to WNW-ESE, with additional N-S-trending faults also present (Nebot, 2016; Nebot and Guimerà, 2016a). These faults define a structural framework of horsts, grabens, and semigrabens. Marked thickness variations occur within the Middle Muschelkalk facies: thicker intervals are associated with downthrown blocks of the acoustic basement, while thinner deposits are found above basement structural highs. The lower part of the Middle Muschelkalk was deposited during active extensional tectonics, whereas the upper part rests atop pre-existing fault basement (Fig. 7A), indicating that the observed thickness variations are primarily of depositional origin.

The upper part of the Middle Muschelkalk evaporites and clays, together with the Upper Muschelkalk carbonates observed in the seismic lines (Fig. 7), exhibit a relatively uniform thickness. This suggests a reduction in normal fault activity within the depocenter of the Triassic Basin. Nevertheless, as previously noted, the basin margins remained controlled by normal faults (Fig. 6). Shortly before and during the sedimentation of the Keuper facies, salt migration within the Middle Muschelkalk led to the development of salt anticlines and welds, resulting in the folding of the Upper Muschelkalk. Consequently, the Keuper facies onlap the folded Upper Muschelkalk, and locally, growth strata are observed within the Keuper succession (Fig. 7B).

Late Jurassic rift configuration

The rocks deposited during this rifting period occupy an area wider than the Maestrat Basin. Structures bounding them can hardly be identified, as they are usually covered by younger rocks. In the northern side of the Maestrat Basin (Figs. 8 and 9), the only Upper Jurassic faults recognized are currently reversed as thrusts. As a result, in the northern thrust-sheet (Calanda Anticline, Fig. 9), only Lower Jurassic rocks are preserved beneath the Albian Utrillas facies. Further south, and north of the Herbers Fault, Upper Jurassic rocks (Polpís Formation) lie unconformably over the Lower Jurassic Cuevas Labradas Formation.

In the Penyagolosa Sub-basin, only the Polpís Formation (Upper Jurassic) is preserved, lying on Triassic rocks, and being covered by the Barremian Camarillas Formation (Fig. 10). Synsedimentary normal faults of decametric dip-slip have been recognized in the center of the basin (Serra d'Esparreguera) in the Bovalar Formation (Upper Jurassic), displaying growth strata in their hanging-wall (Humphrey *et al.*, 2022).

Early Cretaceous rift configuration

The Maestrat and Garraf basins developed during the Late Jurassic-Early Cretaceous. These basins are limited by extensional faults of decakilometric lateral extent and kilometric dip-slip displacement (Nebot and Guimerà, 2016a, b; Marín *et al.*, 2021, 2025; Marín Pérez, 2025; Salas *et al.*, 2001), which can be well identified for the Early Cretaceous.

The Garraf Basin is bounded by NE-SW trending faults, with downthrown hanging walls located to the SE and displacement increasing in that direction. These faults generated several sub-basins, specifically the El Montmell, El Vendrell and Sitges sub-basins, within a basin architecture that exhibits a progressive increase in subsidence from the NW toward the SE (Fig. 2).

As explained above, during the Early Cretaceous extensional phase, the Maestrat Basin was divided into several sedimentary sub-basins bounded by normal faults (Fig. 1). The geological period in which this basin was most clearly defined was during the Barremian and Aptian. During this time, the sedimentary basin was formed by a network of extensional faults oriented approximately E-W, NW-SE, and NE-SW, giving the basin a triangular shape in map view (Fig. 1).

The faults that define the Maestrat Basin are: the Herbers Fault to the north, which connects with the Montalbán Fault, both having a general E-W trend but including inflections where they change to a NE-SW orientation, and the Penyagolosa Fault to the southwest, oriented NW-SE (Fig. 1). Between these two main faults, there are other faults that separate the various sub-basins, chiefly the Xert Fault, oriented E-W, which separates La Salzedella Sub-basin to the south from the Morella Sub-basin to the north, the Aliaga Fault to the north of the Galve Sub-basin, and the Benicàssim Fault, oriented NE-

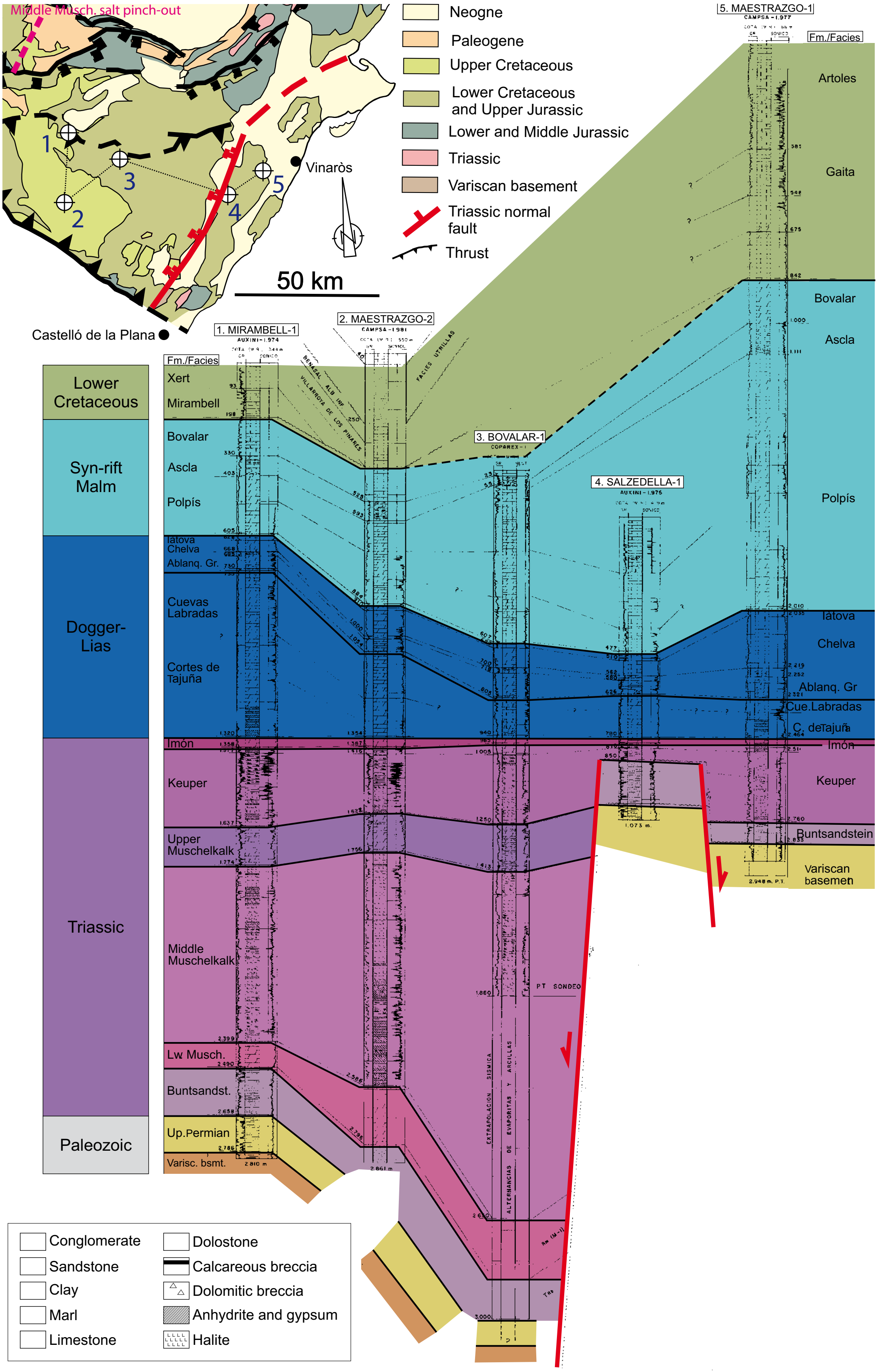

FIGURE 6. Interpretation and correlation of petroleum exploration wells after Martínez-Abad (1991).

SW, which bounded the Orpesa Sub-basin during the late Aptian (Fig. 1). All these faults involve the Variscan basement.

Three geological cross-sections (Figs. 8, 9 and 11), and the corresponding restoration by the end of the Mesozoic, were elaborated to characterize the structure of the Maestrat Basin. Figure 8A shows a reconstruction of the geometry of the Maestrat Basin, after restoring its present-day structure (Fig. 8B) to its state at the end of the Mesozoic. The main sub-basins display the greatest sedimentary thicknesses adjacent to their bounding faults, with thickness progressively decreasing away from these structures. These include: i) the Penyagolosa Sub-basin, bounded to the SW by the Penyagolosa normal fault, and ii) La Salzedella and Morella sub-basins, bounded to the north by the Herbers Fault, but being divided to the SE by the Xert Fault (Fig. 1B). Several secondary faults are present in the hanging-wall of these two main faults.

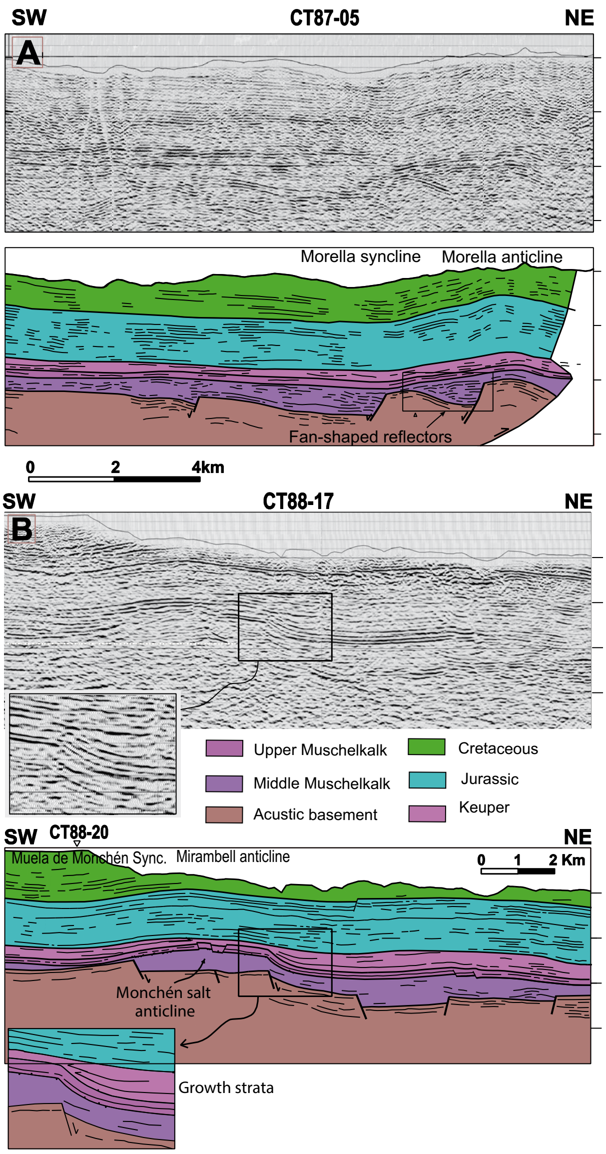

FIGURE 7. Seismic lines depicting the synsedimentary structures present in the Triassic materials (modified from Nebot, 2016). Decoupling of the cover above Middle Muschelkalk evaporites is clearly depicted, as well as drape folds above basement faults. For location, see Fig. 3.

The increase in thickness of the syn-rift rocks toward the bounding faults of the sub-basins (Figs. 1B, 8, 11), indicates that these faults have a listric geometry, that should branch in a basal fault deep in the basement (Fig. 8A). The combination of this fault configuration, Herbers and Xert faults in the north, and Penyagolosa Fault to the southwest, produced a less subsided area, the Vistabella threshold, where a thinner sequence of materials was deposited (Figs. 1B and 2).

The main depocenters are found in the hanging wall of the main bounding normal faults (Fig. 1B). The highest thickness is recorded in La Salzedella Sub-basin, within the hanging-wall of the Xert Fault (Fig. 11A), where approximately 4000m of Upper Jurassic-Lower Cretaceous strata are inferred, compared with ~500m in the footwall to the north. Comparison of Barremian–Aptian successions exposed near the Xert Fault with those farther south indicates the presence of a sedimentary wedge of that age, which thins southward (Fig. 11A). In the Penyagolosa Sub-basin, ~2500m of sedimentary rocks are inferred in the hanging-wall of the fault, versus ~500m in the footwall (Fig. 10). North of the Morella Sub-basin, within the hanging wall of the Herbers Fault, ~2200m of Upper Jurassic–Lower Cretaceous rocks are present, whereas only ~200m occur in the footwall (Fig.12). Farther west, in the Castellote section (Fig. 9), the Herbers Fault juxtaposes ~930m in the hanging wall against ~335m in the footwall, highlighting the overall eastward thickening of the Maestrat Basin. By comparing the present-day structure with its restoration to the end of Mesozoic, the estimated extension during the Lower Cretaceous is 3915m (5%), whereas for the late Permian to Mesozoic period it is 5740m (8%). These values should be regarded as minimum estimates, as decametric- to metric-scale slip normal faults cannot be represented at the scale of the section, despite their widespread occurrence in the Mesozoic record (Nebot, 2016).

The Galve Sub-basin (Fig. 1B) is bounded by the Penyagolosa and Aliaga faults. It contains a thick sedimentary succession of 2300m in their common hanging wall, but only 320m in the footwall of the Aliaga Fault (Guimerà and Salas, 1996). An especial case is the Orpesa Sub-basin (Fig. 1B), which is bounded to the NE by the Benicàssim Fault. In its hanging wall, ~3000m of Upper Jurassic to Lower Cretaceous rocks are present, ~1500m of which belonging to the Benassal Formation, whereas ~1000m of syn-rift rocks are recorded in its footwall (Humphrey *et al.*, 2022; Salas *et al.*, 1995).

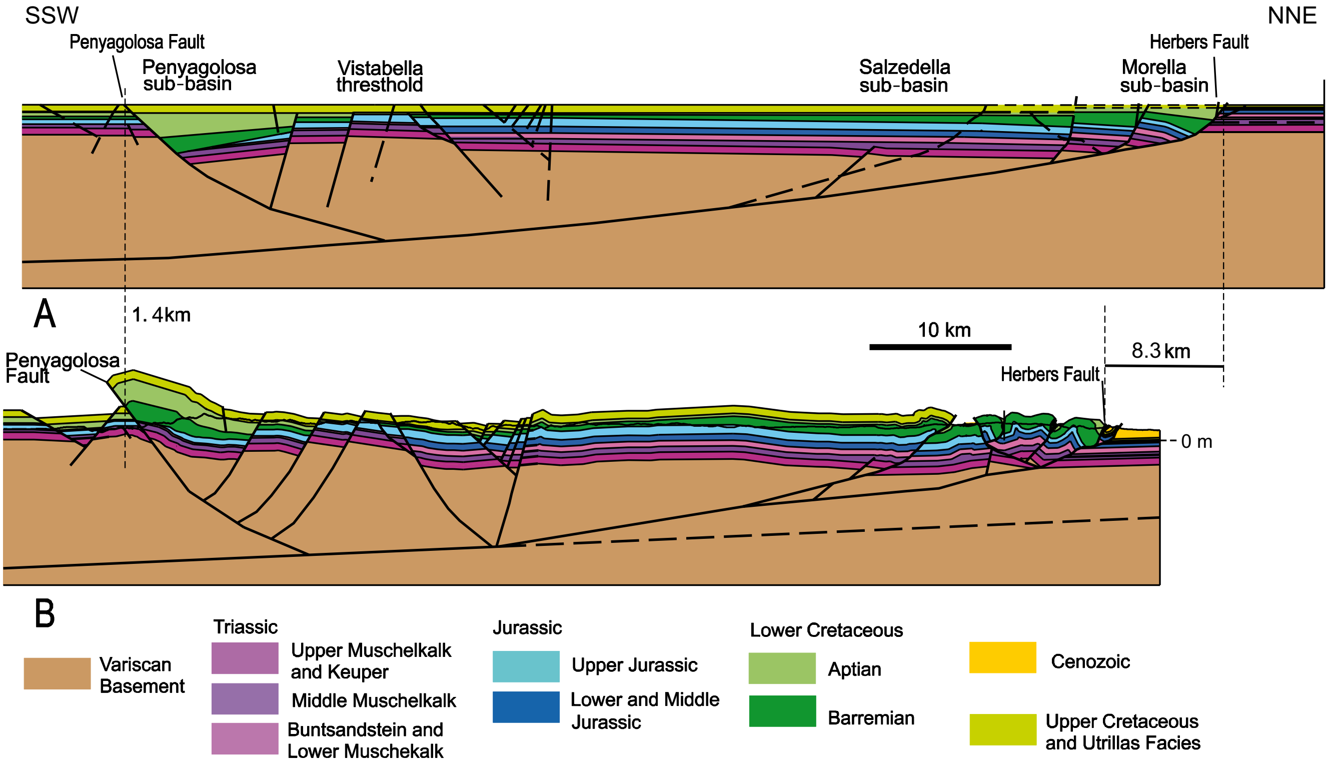

FIGURE 8. Geological section across the Maestrat Basin. A) Its restoration at the end of Cretaceous. B) Present-day geological section. For location, see Fig. 3.

Mesozoic basin evolution

The sedimentary infill of the Upper Jurassic–Lower Cretaceous Maestrat and Garraf basins, along with their Triassic to Middle Jurassic substratum, is subdivided into four major sequences bounded by five regional unconformities (D1-D5; Fig. 4). These major sequences correspond to an updated interpretation of the rifting and post-rift phases associated with the evolution of the Iberian Rift System, as originally proposed by Salas and Casas (1993), Salas *et al.* (2001), Salas *et al.* in Martín-Chivelet *et al.* (2019). This revised framework defines six distinct phases: (i) the late Permian–Middle Triassic Rifting Cycle 1, (ii) the Late Triassic–Middle Jurassic Post-rift Stage 1, including an Hettangian event of rapid syn-rift subsidence, (iii) the Late Jurassic Rifting Cycle 2, (iv) the Neocomian event (late Berriasian–Hauterivian) of decelerated subsidence, (v) the Early Cretaceous (Barremian–early Albian) Rifting Cycle 3, and (vi) the Late Cretaceous Post-rift Stage 2 (Figs. 4 and 5). These evolutionary phases are described in the following subsections.

Late Permian–Middle Triassic Rifting Cycle 1.

The late Permian–Middle Triassic evolution of the Iberian and Catalan-Valencian basins was controlled by crustal extension related to the westward propagation of the Tethys and the southward propagation of the Arctic-North Atlantic rift systems, as well as their interaction within the North Atlantic-Iberian domain (Ziegler, 1988). The basement faults that define these basins (Esteban and Robles, 1979) likely resulted from the extensional reactivation of the late Hercynian shear zones (Arthaud and Matte, 1977; Capote, 1983; Vegas and Banda, 1982). The Triassic succession attains thicknesses of up to 1200m (Virgili *et al.*, 1983).

In the Maestrat Basin, the first stage of extensional activity (late Permian–Ladinian) led to the development of a high-angle normal fault system that fragmented the Variscan basement into a system of horsts, grabens and half-grabens (Nebot and Guimerà, 2016c). These faults were active during the deposition of the upper Permian red beds and the Buntsandstein facies, persisting until the deposition of lower part of the Middle Muschelkalk facies. This prolonged tectonic activity progressively infilled the fault-controlled topography, generating significant variations in depositional thickness. The fault system was overstepped by the upper part of the Middle Muschelkalk, marking a decline in extensional activity that continued until the deposition of the Upper Muschelkalk carbonates, which exhibit a nearly uniform thickness (Fig. 7). However, subsidence curves indicate that Rifting Cycle 1 persisted until the Ladinian Upper Muschelkalk (Fig. 5). Accordingly,

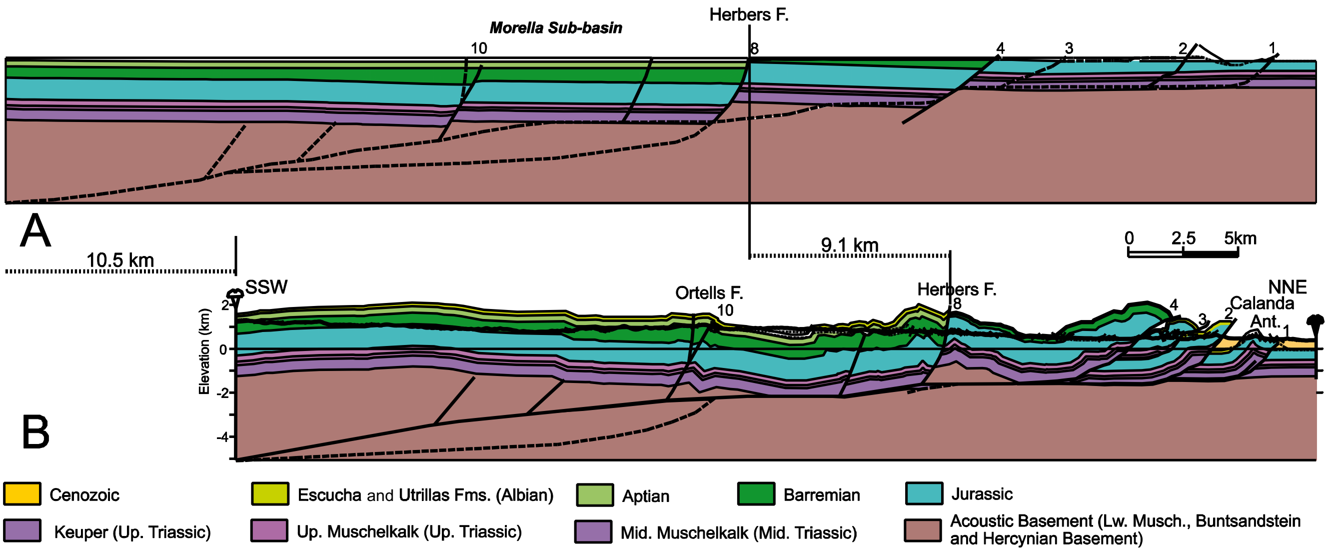

FIGURE 9. Geologic section across the Castellote area (modified after Nebot, 2016). A) Its restoration at the end of Cretaceous. B) Present-day geological section. For location, see Fig. 3.

Post-rift Stage 1 is considered to begin with the deposition of the Upper Triassic Keuper facies. A similar pattern is observed in subsidence curves for the late Permian–Triassic interval calculated in the Iberian and Ebro basins by Arche *et al.* (2004). In the Triassic Catalan basin, the Ladinian stage was a period of widespread and rapid syn-rift subsidence where extensive carbonate successions deposited at this time (Mercedes-Martín *et al.*, 2014a, b; Tucker *et al.*, 1993).

Late Permian and Early Triassic sedimentation began under continental conditions within isolated grabens, which later coalesced. The fluvial red beds of the Buntsandstein facies, which onlap the D1 unconformity, reach thicknesses of up to 600m. In its upper parts, the Buntsandstein includes thick Anisian anhydrites and salts, particularly in the central part of the study area (Fig. 3). Toward the southeast and east, these evaporites and red beds grade into the carbonates of the Muschelkalk facies, reflecting the transgression of the Tethys Sea. The Lower Muschelkalk (Anisian in age) and the Upper Muschelkalk (Ladinian) are separated by basal Ladinian shales and evaporites. Combined, these carbonate units reach thicknesses of up to 300m in the Catalan Coastal Chain and the València Basin.

By the time the upper part of the Buntsandstein was deposited, the Catalan-Valencian and Iberian rift systems were well established, with the latter extending from the València-Maestrat area to Cantabria, where it linked with the evolving Bay of Biscay rift. Despite this connectivity, Middle Triassic transgressions (Calvet *et al.*, 1990) do not appear to have progressed northwestward across the rift shoulder of the Bay of Biscay (Arche and López-Gómez, 1996; Sopeña *et al.*, 1988). Throughout the Triassic, sedimentation broadly overstepped the margins of the rifted Iberian basins, driven in part by rising eustatic sea levels (Haq *et al.*, 1987, 1988) and possibly also by shallow lithospheric necking levels (Kooi *et al.*, 1992).

Late Triassic–Middle Jurassic Post-rift Stage 1

Carnian and Norian strata, up to 200m thick, mark the beginning of the Post-rift Stage 1 and are represented by typical evaporitic and red-bed deposits of the Keuper facies (Ortí-Cabo, 1982-83). During the deposition of the Keuper facies, however, the reactivation of certain normal faults within the acoustic basement (upper Permian–Lower Muschelkalk) triggered the Middle Muschelkalk salt flow (Fig. 7B). This process led to the formation of salt anticlines and welds, increasing depositional thickness variations within the Keuper facies.

The Rhaetian consists of dolostones that grade laterally into evaporites (Arche and López-Gómez, 1996; Sopeña *et al.*, 1988). Accordingly, by Late Triassic, much of eastern and southeastern Iberia was submerged beneath a broad basin that formed part of the Peri-Tethyan platform. Furthermore, volcanic rocks of both tholeiitic and alkaline affinities were also extruded during the Middle and Late Triassic.

At the end of the Triassic, and prior to the deposition of the Liassic platform carbonates, a significant rifting event affected the Iberian Basin (Fig. 5). Locally, Hettangian breccias unconformably overlie a truncated and tilted Triassic succession (Aurell *et al.*, 1992; Campos *et al.*, 1996; Guimerà, 1988; Roca and Guimerà, 1992; Roca *et al.*, 1994; San Román and Aurell, 1992), marking the D2 unconformity (Fig. 4). These breccias, which constitute the Cortes de Tajuña Formation, recorded a tectonically driven collapse of carbonate platforms, resulting from extensional

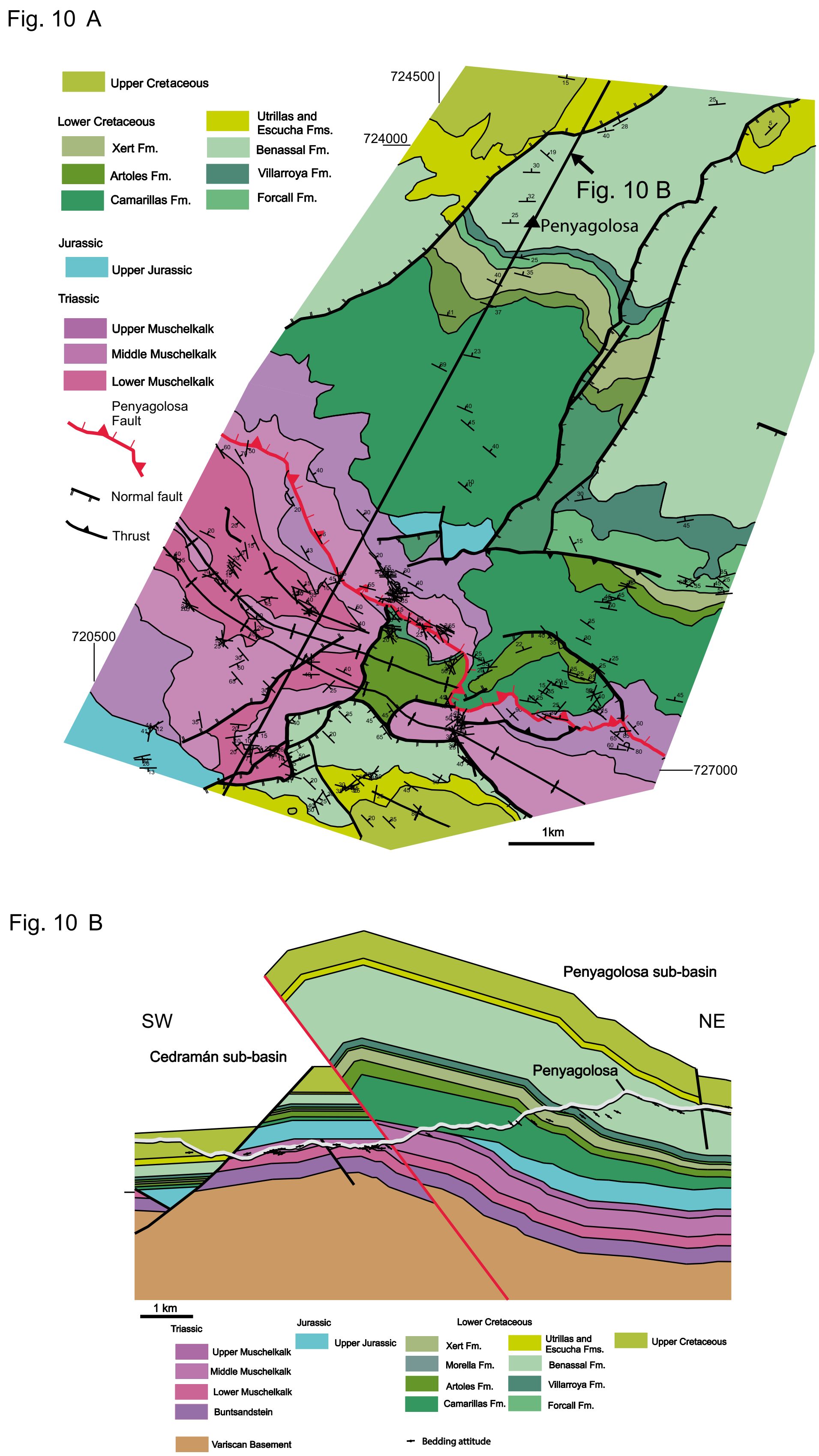

FIGURE 10. Detailed geologic map (A) and geologic section (B) of the Penyagolosa area. For location, see Fig. 3.

tilting of fault blocks and related footwall uplift. From the elevated margins of the footwall blocks, sedimentary breccias were shed into adjacent, rapidly subsiding hanging wall blocks, where interfinger with thick dolomite and evaporite units. Pre-Jurassic erosion and extensional tilting of basement blocks generated angular unconformities between the Jurassic and underlying Keuper or uppermost Muschelkalk units in the Catalan Coastal Chain (Esteban and Julià, 1973), and between the Jurassic and the top of the Buntsandstein in the eastern Iberian Chain, notably in Cedrillas-Corbalán and Desert de les Palmes areas (Aurell *et al.*, 1992; Roca and Guimerà, 1992). The Hettangian continental rifting event (Figs. 4 and 5) was also recognized in the Lusitanian basin by Stapel *et al.* (1996) and could be related to the onset of rift systems in the Central Atlantic-Alpine domain and the opening of the Neotethys (Stampfli and Kozur, 2006).

However, considering the brief Hettangian subsidence pulse, characterized by block rotation, erosion, and the development of the basal erosional surface D2, within a broader post-rift interval, an alternative interpretation involving salt tectonics may be considered. These features could also be consistent with the extension of a thin overburden over a mobile detachment. Indeed, Vendeville and Jackson (1992) describe examples of reactive diapirism initiated by slow regional extension rates.

In contrast to the South Iberian margin and the Bay of Biscay, where continued rifting controlled Jurassic evolution (Le Vot *et al.*, 1996; Vera, 2001), the Early to Middle Jurassic development of the Catalan-Valencian and Iberian rift systems were mainly controlled by thermal subsidence (Fig. 5). This period of relative tectonic quiescence favored the establishment of extensive carbonate platforms passing basinwards to deeper marine marls (Fig. 4) that overlain pre-existing extensional structures (Salas *et al.*, 2001, 2010). In certain areas, such as the Desert de les Palmes, north of Castelló de la Plana (Fig. 6), the Lower and Middle Jurassic succession directly overlies Buntsandstein facies (Guimerà, 1988; Roca *et al.*, 1994).

During the deposition of the Sinemurian to Oxfordian successions, minimal fault activity resulted in the progressive overstepping of the basin margins. However, unlike the typical evolution of post-rift thermal sag basins, Pliensbachian to Bajocian volcanic activity occurred along the western margin of the study area (Lago *et al.* in Vera, 2004; Martínez *et al.*, 1997; Vera, 2001).

The Sinemurian–Carixian carbonate platform (Fig. 4) is extensively dolomitized in the northern part of the Catalan Coastal Chain, particularly in the Garraf and Montmell massifs (Fig. 1). An intra-Sinemurian erosional unconformity in this area separates a basal dolomitic-breccia from an overlying succession of a thin terrigenous siliciclastic interval and thick Upper Jurassic dolomites (Esteban, 1973; Salas, 1987). In contrast, Domerian to Toarcian successions elsewhere are characterized by pelagic marls containing open marine biota, such as ammonites. The Aalenian to Oxfordian interval includes successions of monotonous nodular ammonite-bearing carbonates, as well as limestones with sponges and microbial filaments, all of which exhibit a clear Tethyan faunal affinity (Bulard, 1972; Canérot, 1991; Fernández, 1985; Gómez, 1979).

Lower and Middle Jurassic strata reach thicknesses of up to 1km, with notable thickness variations observed within the early Lias. At least eight lower-rank depositional sequences can be consistently correlated across the basin. The unconformities bounding these sequences align more closely with the supercycles of the Exxon global sea-level curve than with its third-order cycles (Aurell, 1990; Giner, 1980; Salas, 1987; Salas *et al.*, 1992). During the Middle Jurassic, a paleotopographic high in the central Iberian Chain caused localized variations in the regional facies distribution. In contrast, the Garraf Basin records a significant stratigraphic gap, with the late Pliensbachian to Oxfordian interval notably absent (Salas, 1987).

Late Jurassic Rifting Cycle 2.

The Late Jurassic rifting cycle extended from the Kimmeridgian to the middle Berriasian and coincided with the northward propagation of rifting from the Central Atlantic into the North Atlantic domain, ultimately leading to the gradual opening of the oceanic North Atlantic Basin (Le Vot *et al.*, 1996; Vergés and Garcia-Senz, 2001; Ziegler, 1988). This period was marked by intense rifting activity in the North Atlantic domain, particularly in the Lusitanian Basin (Pimentel and Pena dos Reis, 2016). Meanwhile, along the South Iberian margin, a transform margin regime began in the Oxfordian and persisted until the Aptian (Vera, 2001). In contrast, Pedrera *et al.* (2020) characterized the South Iberian rifted margin as oblique, featuring rift segments partitioned by transfer faults. In this region, rifting persisted into the Albian.

In the Iberian Basin, this rifting cycle led to the progressive dismantling of the Lower and Middle Jurassic carbonate platforms and the initiation of a new system of extensional basins, including the Cameros, Maestrat, Columbrets, and South Iberian basins (Salas *et al.*, 2010). These Upper Jurassic basins are discordantly superimposed on the older Triassic Iberian rift structures. The sedimentary and structural records preserved within them allow for the recognition of at least four distinct depositional sequences (Salas *et al.*, 2001).

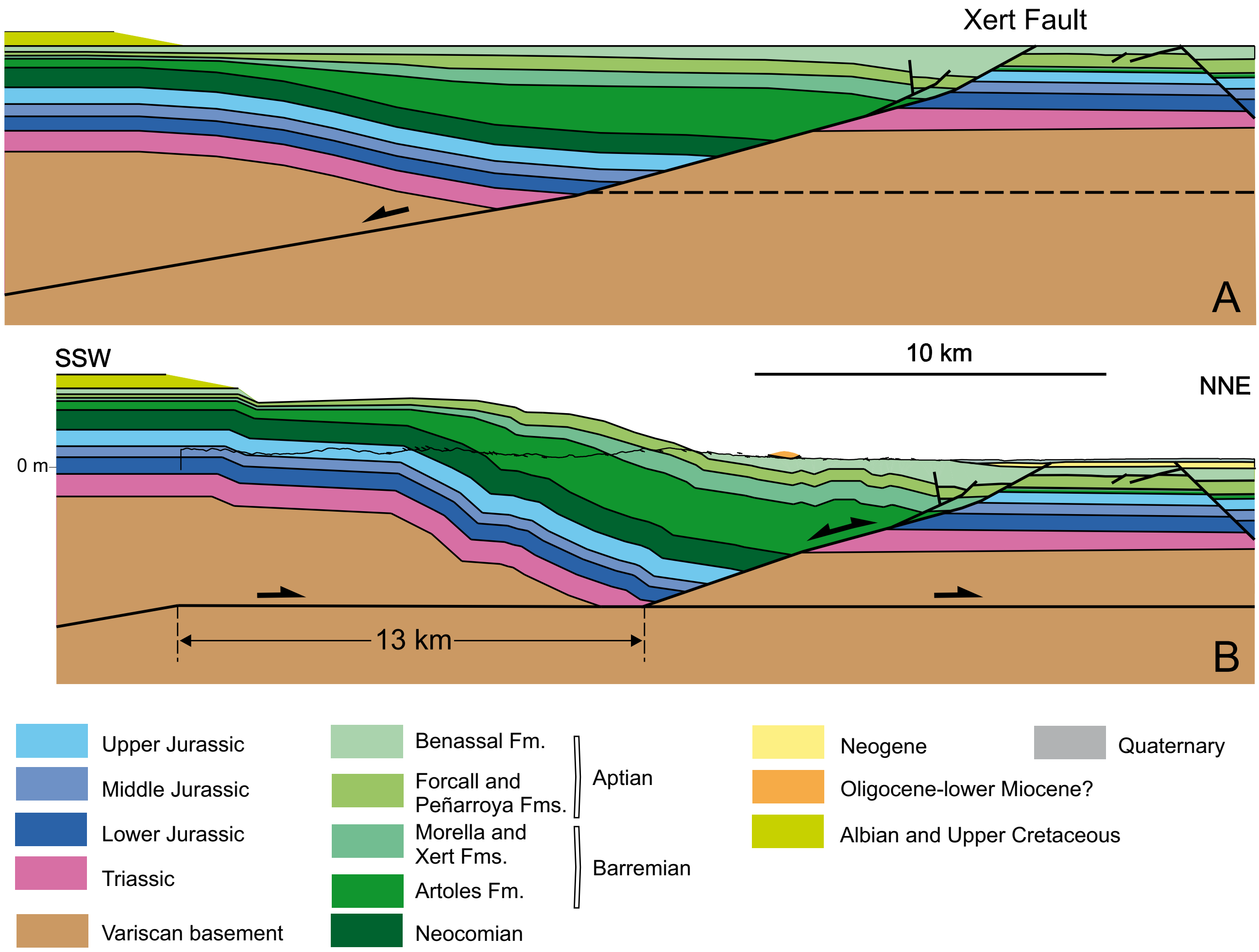

FIGURE 11. Geological section across the La Salzedella Sub-basin depocenter. A) Restoration at the end of the Cretaceous. B) The present-day cross-section (at the SSW end, the Neogene SE tilting of bedding was removed). 13 km of thrust-sheet displacement is deduced, which was transferred to thrusts to the North. For location, see Fig. 3.

Syn-rift subsidence commenced in the Maestrat Basin during the earliest Kimmeridgian and in the Cameros Basin during the early Tithonian. The syn-rift sedimentary infill of these basins reaches thicknesses of up to 5km and is bounded by two major unconformities. In the Cameros Basin, the basal unconformity represents a stratigraphic gap spanning from the early Tithonian to the Barremian (Mas *et al.*, 1993), whereas in the Maestrat Basin, this gap is considerably narrower, affecting only the upper part of the latest Oxfordian Planula ammonite biozone (Aurell, 1991). The upper boundary of the syn-rift succession is marked by a prominent intra-Berriasian unconformity (D3), which preceded the onset of the Neocomian event of decelerated subsidence (Figs. 4 and 5).

In the Maestrat Basin, the Late Jurassic syn-rift depositional system was dominated by shallow marine carbonates (Fig. 4; Salas *et al.*, 1995). The onset of rifting coincided with a major sea-level rise, which, combined with rapid subsidence of tilted blocks, led to the drowning of a c. 50m thick, shallow-water Oxfordian sponge-rich carbonate ramp. This was followed by the deposition of up to 800m thick limestones of the Kimmeridgian Polpís Formation, including anoxic basinal marls (Ascla Formation) in the evolving hangingwall blocks. Laterally, these deposits transition into thin-bedded lime mudstones and sponge buildups (Salas and Casas, 1993). Geochemical analyses of minerals and organic matter from the Ascla Formation, along with oil shows in the Maestrazgo-1 well and Amposta field, confirm that the Ascla Formation constitutes the source rock for the Amposta oil (Permanyer and Salas, 2005; Rossi *et al.*, 2001; Salas and Permanyer, 2003). The overlying Tithonian to Berriasian succession comprises a variety of carbonate platform depositional settings, including tidal flats and fringing oolitic-bioclastic shoals, which grade basinward into hemipelagic Calpionella limestones, reaching thicknesses of up to 1000m.

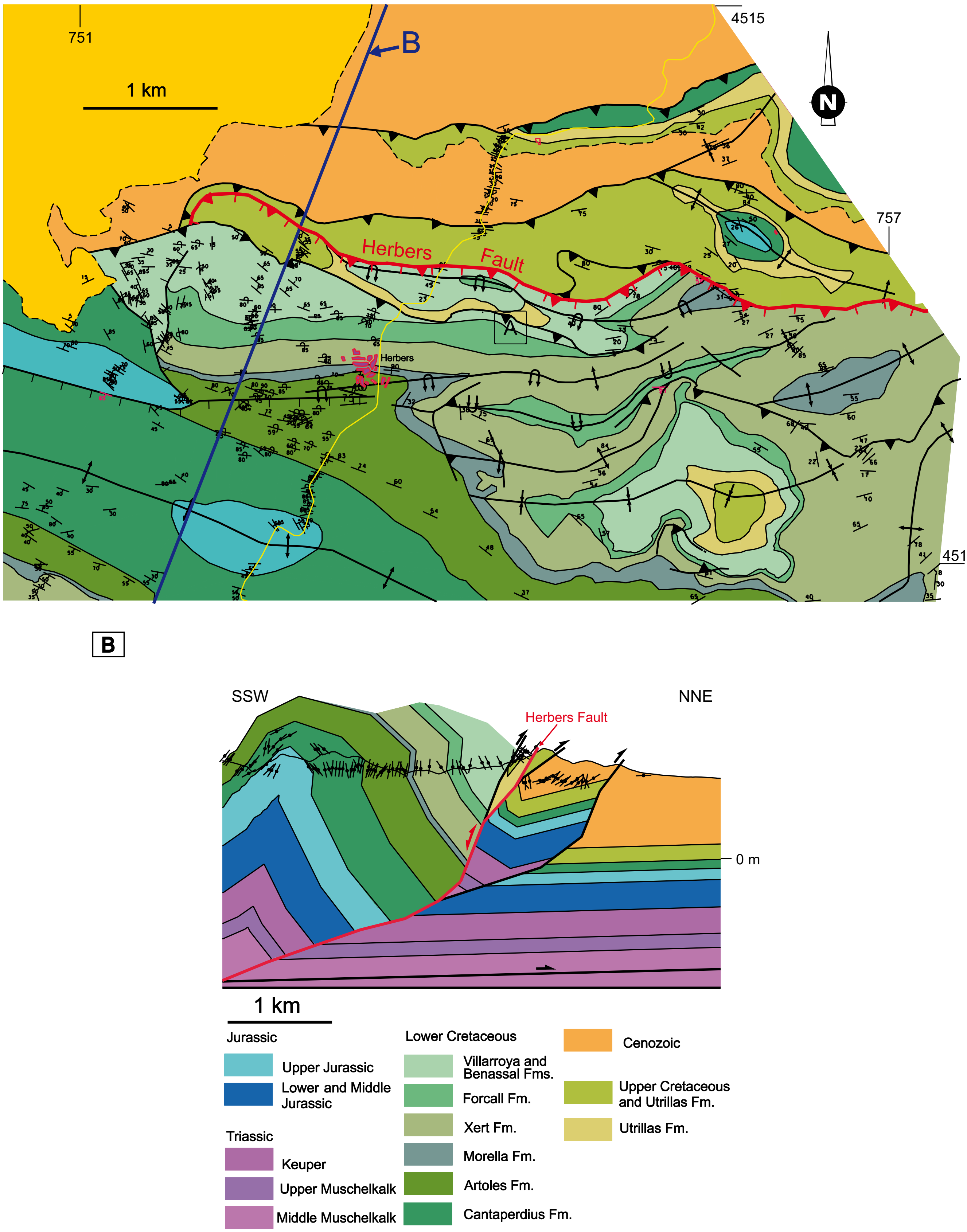

FIGURE 12. Detailed geologic map (A) and geologic section (B) of the Herbers area. For location, see Fig. 3.

DOI: 10.1344/GeologicaActa2026.24.9

Neocomian event

The Neocomian event in the Maestrat Basin began during the late Berriasian and ended in the Hauterivian (Figs 4 and 5). This interval was marked by relative tectonic quiescence and decelerating subsidence. In large areas of the Maestrat and Garraf basins, the Neocomian record is absent, and basal Barremian deposits rest unconformably (D3) on the eroded Jurassic substratum. As a result, Barremian units locally overlie Jurassic formations directly. In the Garraf Basin and the northern part of the Maestrat Basin, upper Berriasian to Hauterivian strata were either not deposited or subsequently eroded, producing a stratigraphic hiatus of this age (Salas, 1987; Salas *et al.*, 2001).

In the Maestrat basin, marine Neocomian sedimentation, reaching thicknesses of up to 775m, was largely confined to the depocentral parts of the sub-basins. In contrast, freshwater carbonates of the Herbers and Mangraners formations were deposited in marginal settings, exceptionally, within the depocenter of La Salzedella Sub-basin during the early Valanginian.

Overall, the Neocomian sedimentary record in the La Salzedella and Morella sub-basins indicates a brackish estuarine environment, represented by the Mangraners, Polacos, Bastida, Llàcova, and Herbers formations (Fig 4), with significant freshwater discharges recorded in the Mangraners and Herbers formations. Shallow marine carbonate production, associated with the Polacos, Bastida, and Llàcova formations, was dominated by molluscs, calcareous algae, benthic foraminifera such as Valdanchella miliani (early Valanginian), and small requienid rudists. Marginal oolitic-bioclastic shoals and coralgal boundstones were also abundant. During the Hauterivian, deeper marine basinal marls with ammonites of the Gaita Formation were restricted to the depocentral area of the La Salzedella Sub-basin (Fig. 1B; Garcia *et al.*, 2014). In the Garraf basin the Neocomian succession (Fig. 4) comprises up to 50m of freshwater carbonates from the Mangraners Formation, overlain by up to 150m of shallow marine limestones from the Polacos Formation, also dominated by Valdanchella miliani, dasycladacean algae, and small requienid rudists.

In the Galve and Penyagolosa sub-basins, located in the westernmost part of the Maestrat Basin (Fig. 1B), Neocomian sedimentation was dominated by siliciclastic deposits comprising two main lithostratigraphic units: Mora and El Castellar formations (Fig. 4). The Mora Formation, dated to the upper Berriasian–Valanginian and reaching up to 140m in thickness, consists of white sandstones interbedded with red shales, interpreted as fluvial to transitional deposits. The overlying El Castellar Formation, Valanginian to middle Hauterivian in age and 80-140m thick, is made up of green shales and sandstones deposited in a muddy alluvial plain with channels, capped by lacustrine limestones (Caja *et al.*, 2007). In the Galve sub-basin, Aurell *et al.* (2016) proposed two new lithostratigraphic units, likely equivalent to the Mora Formation, named the Aguilar de Alfambra and Galve formations, deposited in transitional coastal plane to restricted lagoon settings and in alluvial floodplain environments, respectively, with a combined thickness of up to 350m.

Early Cretaceous Rifting Cycle 3

Rifting resumed during the Barremian and persisted until the early Albian, coinciding with the gradual opening of the oceanic North Atlantic Basin. The onset of seafloor spreading in the Bay of Biscay–Pyrenean domain was diachronous. In the Western Galicia Bank, it commenced after the M0 magnetic anomaly, which marks the base of the Aptian. On the Asturian margin and the Le Danois Bank, proto-oceanization began during the early Albian (Madarieta Txurruka *et al.*, 2025). Conversely, the Basque–Cantabrian Basin and the Pyrenean paleorift represent failed rifts where mantle exhumation ceased in the early Cenomanian without progressing to full oceanization (Pedrera *et al.*, 2021). The Late Jurassic transtensional rifting in the Bay of Biscay culminated in mid-Aptian crustal separation and the onset of sea-floor spreading (Tugend *et al.*, 2015; Vissers and Meijer, 2012). In the Maestrat and Garraf basins, intraplate extension peaked during the Early Cretaceous, in marked contrast to the limited coeval extension recorded at the Atlantic margin, which was undergoing thermal subsidence at that time. The initial syn-rift deposits grade from restricted marine to lacustrine and alluvial environments. These include significant volumes of freshwater carbonates of the Cantaperdius Formation and siliciclastic supplies deposited in embayment and estuarine settings, corresponding to the Weald facies and represented by the Camarillas and Mirambell formations (Fig. 4).

The upper part of the Barremian succession, reaching thicknesses of up to 1100m, includes the shallow-marine carbonates and marls rich in oysters of the Artoles Formation, the continental red clays and sandstones containing dinosaur remains of the Morella Formation, the coastal mixed carbonate-siliciclastic deposits of the Cervera del Maestrat Formation, and the marine sandstones, sandy limestones, marls and limestones rich in Palorbitolina lenticularis of the Xert Formation (Fig. 4; Bover-Arnal *et al.*, 2016).

From oldest to youngest, the uppermost Barremian–lowermost Albian succession (up to 650m thick) comprises: i) the basinal marls, marly-limestones and limestones with Palorbitolina lenticularis and ammonoids of the Forcall Formation, ii) the platform carbonates with rudists and corals of the Villarroya de los Pinares Formation, and the marls and limestones with rudists, corals and Mesorbitolina texana of the Benassal Formation (Fig. 4; Bover-Arnal *et al.*, 2014, 2016; Canérot *et al.*, 1982; Salas, 1987; Salas *et al.*, 1992). The thickness of the Benassal Formation varies significantly, ranging from 80-200m to nearly 1500m in the Orpesa sub-basin (Fig. 1B; Martín-Martin *et al.*, 2013; Roca and Guimerà, 1992; Roca *et al.*, 1994; Salas, 1987). The Benassal Formation is overlain by the lower Albian sandstones and clays of the Escucha Formation (Bover-Arnal *et al.*, 2025; Moreno-Bedmar *et al.*, 2008), deposited in a widespread tidally-influenced deltaic system. This formation reaches thicknesses of up to 500m and contains thick coal layers (Querol *et al.*, 1992).

Late Cretaceous Post-rift Stage 2

During the Late Cretaceous, the Iberian Peninsula constituted a separate tectonic plate, as the result of its rifting from Europe since the late Permian and its ~35° counter-clockwise rotation during the Aptian (Vissers and Meijer, 2012). The separation of the Iberian Plate from Europe was a diachronous process spanning the latest Tithonian to the early Cenomanian. Break-up at the southernwestern corner of Iberia is dated to the late Tithonian in the Gorringe Bank (Pedrera *et al.*, 2021), whereas in the Basque–Cantabrian Basin and the Pyrenean paleorift, it was completed by the early Cenomanian. The Iberian continental block was flanked by passive margins facing the Tethys and the North Atlantic. Its northern margin underwent accelerating extension from the late Aptian to the early Cenomanian. This passive-margin stage persisted until the early Santonian, followed by the onset of the Alpine orogeny in the late Santonian. During the Paleogene, the Alpine orogeny exerted a contractional tectonic regime along the Tethyan margin of Iberia (Le Vot *et al.*, 1996; Tavani *et al.*, 2018; Tugend *et al.*, 2015; Vissers and Meijer, 2012; Ziegler, 1988).

Following the final rifting pulse in the early Albian, the Iberian Basin entered a phase of tectonic quiescence. From that point until the Maastrichtian, its evolution was mainly controlled by lithospheric thermal relaxation and eustatic sea-level rise. As a result of the overall Late Cretaceous transgression, extensive shallow-marine carbonate platforms developed across large areas of northwestern Iberia (Alonso *et al.*, 1993; Haq *et al.*, 1987, 1988), punctuated by short-lived sea-level falls and episodes of continental sedimentation (*e.g.*, Martín-Closas *et al.*, 2025).

Throughout most of the study area, the base of the middle Albian to Upper Cretaceous major sequence lies unconformably (D4) over Aptian, Barremian, Neocomian, Jurassic, Triassic, and Paleozoic strata, as well as metamorphic and igneous rocks. This stratigraphic complexity beneath the middle Albian is not illustrated in Figure 4, in order to maintain visual clarity, avoid overcomplicating the stratigraphic depiction, and focus on the main depositional trends. The D4 unconformity is onlapped by the fluvial siliciclastic Utrillas Formation, a homogeneous yet diachronous unit ranging in age from the middle to late Albian (Fig. 4). During the Cenomanian transgression, an extensive carbonate platform developed, linking the Atlantic and Tethys domains. The overlying Turonian–Coniacian succession begins with pelagic carbonates that transition upward into thick dolomitic facies. The Senonian succession exhibits a pronounced shallowing-upward character, transitioning from open marine enviornments to sublittoral, lagoonal, and ultimately freshwater carbonate settings. Aurell *et al.* (2022) described the Allueva Formation as a new lithostratigraphic unit within Las Parras Sub-basin (Fig. 1B). This continental unit, locally reaching up to 70m in thickness, is dated to the middle–late Campanian. The Upper Cretaceous lithostratigraphic units progressively onlap toward the NW (Canérot *et al.*, 1982; Floquet *et al.*, 1982; García-Mondéjar, 1989; Viallard, 1973). This Upper Cretaceous major sequence is up to 500m thick in the Maestrat Basin and 250m in the Garraf Basin. It can be subdivided into twelve transgressive-regressive depositional sequences, which in turn can be grouped into four second-order cycles or megasequences (Alonso *et al.*, 1993). Most of these sequences correlate well with those of the Exxon sea-level curve.

Cenozoic contractional inversion

From the Late Cretaceous onwards, the convergence between the African and Eurasian plates caused crustal contraction. As a result of this, some of the normal faults that had defined the Maestrat Basin were inverted and became thrust faults; moreover, new thrusts were also generated. As a result, a belt of folds and thrusts developed, known as the Linking Zone between the Iberian Chain and the Catalan Coastal Chain (Guimerà, 1983, 1984, 1994; Fig. 3). This deformation mainly took place between the late Eocene and the Early Miocene (González *et al.*, 1998; Guimerà, 2004, 2018), although evidence of local deformation of Late Cretaceous age has been recognized NW of Montalbán (Aurell *et al.*, 2022).

The Linking Zone is a triangular-shaped unit located in the area where the major NE-SW and NW-SE basement faults of the Catalan Coastal and Iberian chains intersect. Its structure is strongly influenced by the Mesozoic normal faults that originally formed the Maestrat Basin. The northern margin of the Linking Zone consists of a thrust and fold belt, oriented approximately E-W, with two inflections where it trends more NE-SW. This belt extends from Portalrubio (in Aragón, north of Teruel) to

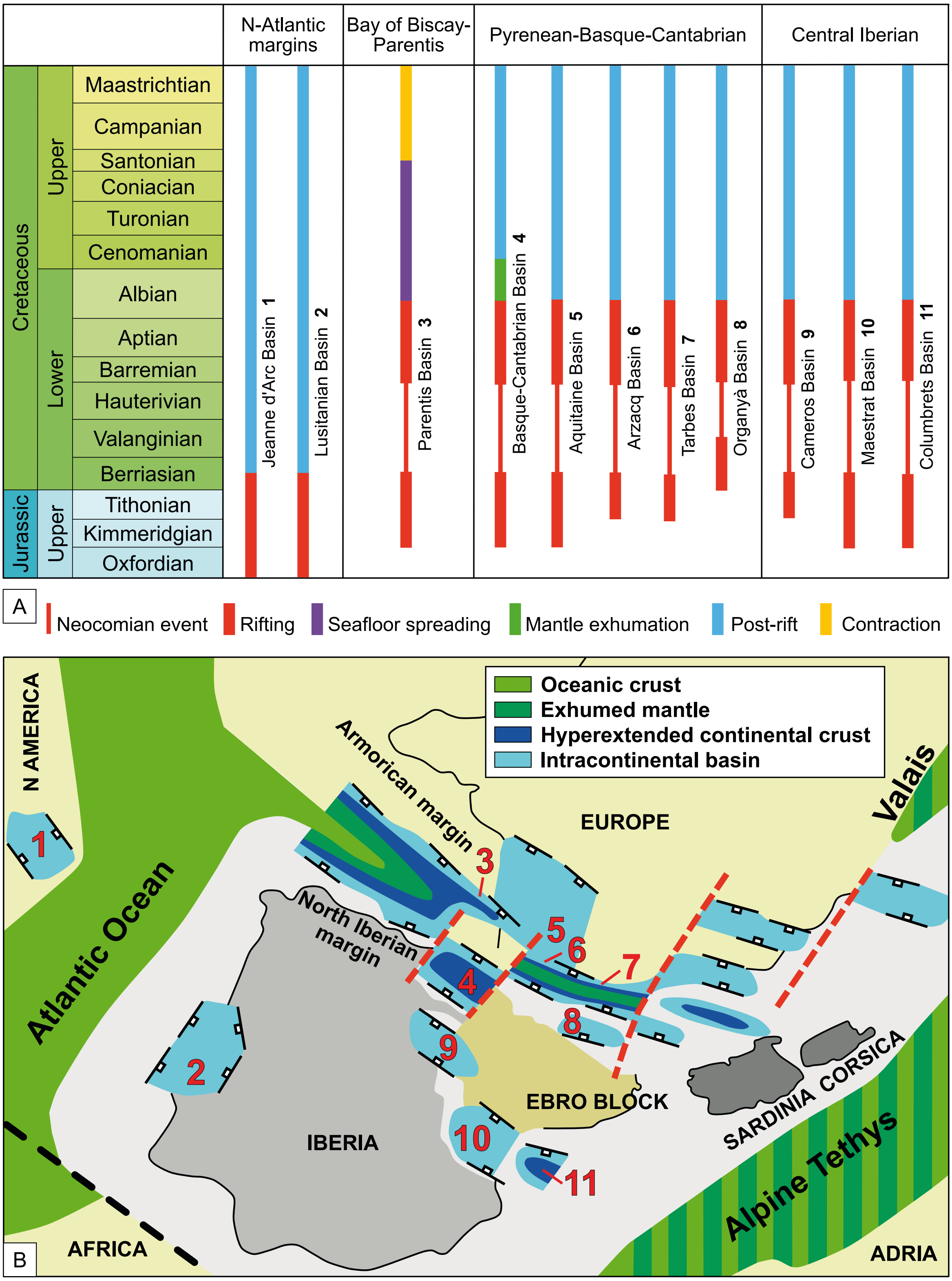

FIGURE 13. A) Table summarizing the Late Jurassic–Cretaceous deformation history of the Central Iberian Rift System. The North Atlantic, Bay of Biscay-Parentis, and Pyrenean-Basque-Cantabrian rift systems reviewed in this work are also indicated. Data compiled from Asti et al. (2022), Borel (1997), Etheve et al. (2018), Pimentel and Pena dos Reis (2016), Ramos et al. (2023), Salas and Casas (1993), Salas et al. (2001), Salas et al. in Martín-Chivelet et al. (2019), Stampfli (2000), Stampfli et al. (2002), Tavani et al. (2018), and Tugend et al. (2015). B) Schematic reconstruction of the Iberia-Eurasia and North Atlantic margins, and adjacent areas during mid-Cretaceous times, showing the main basins. Modified from Tavani et al. (2018).

the Catalan Mediterranean coast at Vandellós (Fig. 3). Due to the movement along these thrusts, the Mesozoic cover was displaced northward, placing the materials that form the Linking Zone above the structures of the Iberian Chain, the Ebro Basin, and the Catalan Coastal Chain. South of the thrust and fold belt, deformation progressively diminishes, transitioning into a slightly deformed area where the strata remain nearly horizontal, only occasionally affected by minor folding.

The Cenozoic horizontal shortening, calculated from the section shown in Fig. 7 between the inverted Penyagolosa and Herbers faults, is 9.3km: 8.3km of reverse displacement along the Penyagolosa and Herbers fauts, plus internal deformation within the thrust sheet (Fig. 8), and an additional 1km resulting from the inversion of the three thrusts north of the Herbers Fault (Fig. 12 B). In this section, the thrust-system north of the Herbers Fault is not represented because it is covered by unconformable Cenozoic. In the section shown in Fig. 9, thrusts north of the Herbers Fault were characterized, and a horizontal shortening of 9.1 km was deduced. Hence, a total horizontal shortening of 18.4 km can be inferred by combining these two sections, between the inverted Penyagolosa Fault and the northernmost thrust of the Linking Zone.

Accordingly, the Cenozoic contractional thrust system appears to be strongly influenced by the pre-existing Mesozoic extensional faults. Two interpretations are proposed: i) complete coincidence of the basal fault in both systems, as proposed in Fig. 2; or ii) partial coincidence, with the Cenozoic basal thrust locally truncating the Mesozoic basal extensional fault (Fig. 9), as interpreted by Nebot (2016) and Nebot and Guimerà (2016b, d), both resulting in a similar surficial structure that forms the Calders Monocline through up-ramp thurst-sheet displacement.

DISCUSSION

Controls on sedimentation and accommodation.

The main control on sediment distribution, facies development, and sedimentary environments was the structural configuration of the rift basin margins. This structural arrangement created differences in accommodation in footwall and hanging wall settings. In some parts of the basins, particularly during the Aptian, climate-induced base-level changes also caused carbonate platform segmentation, progradation, incision, and retrogradation (Bover-Arnal *et al.*, 2009, 2014, 2015, 2022, 2024). Variations in accommodation are also important because, under similar climatic and lithological conditions, the size of a drainage basin controls freshwater and sediment discharge at its outlet. This, in turn, affects the development and extent of alluvial fans and fan deltas along graben margins. This control becomes particularly significant during the Barremian in the Galve and Penyagolosa sub-basins, where the Weald facies, represented by the Mora, Castellar and Camarillas formations, accumulated (Caja *et al.*, 2007; Liesa *et al.*, 2006; Navarrete *et al.*, 2013). Accommodation also varies depending on the relative position within each tilted semigraben. In the Maestrat Basin, La Salzedella and Penyagolosa sub-basins contain the thickest Upper Jurassic–Lower Cretaceous syn-rift successions, up to 4.3km and 2.5km, respectively, adjacent to their bounding Xert and Penyagolosa master faults. Stratal geometries in these sub-basins typically display wedge-shaped patterns that thin toward the uplifted shoulders and the Vistabella threshold (Fig. 2A). Similarly, the Sitges Sub-basin is the most subsiding semigraben in the Garraf Basin, accumulating more than 2.2km of sediments near El Vendrell Fault (Fig. 2B).

Mesozoic plate tectonics

Evidence from biota and sedimentary facies indicates that, since the Late Jurassic, the Iberian Basin was connected to the Alpine Tethyan domain (Mas *et al.*, 1993; Salas and Casas, 1993; Salas *et al.*, 2001). Alvaro *et al.* (1979) interpreted the Iberian Basin as an aulacogen, a failed rift arm of a triple junction associated with the Alpine Tethys. The diachronous onset of syn-rift subsidence indicates that the Iberian Basin may have propagated toward the northwest.

Plate tectonic reconstructions suggest that the late Permian to Hettangian evolution of the rifted Iberian Basin was driven by the westward propagation of the Tethys and the southward propagation of the Arctic-North Atlantic rift systems, as well as by their interaction within the Iberian-North Atlantic domain. The Late Jurassic to Early Cretaceous rifting cycles in the Iberian Basin coincided with the progressive opening of the North Atlantic and with sinistral oblique extension within the Bay of Biscay rift, preceding the mid-Aptian crustal separation between Iberia and Europe. Rifting activity persisted in the Iberian Basin during the initial stages of seafloor spreading in the Bay of Biscay and only ceased in the early Albian. Crustal separation along the North-Iberian margin was diachronous, with final separation between the Iberia and Eurasia plates achieved in the early Cenomanian (Pedrera *et al.*, 2021).

Recent plate-kinematic reconstructions (Nirrengarten *et al.*, 2018; Tugend *et al.*, 2015) partition Late Jurassic–Early Cretaceous deformation between Iberia and Eurasia among three transtensional trough corridors corresponding to the principal rift systems: the Iberian basin, the Pyrenean-Basque-Cantabrian, and the Bay of Biscay-Parentis, separated by two intervening microcontinental blocks (the Landes High and the Ebro Block).

During the Late Cretaceous Post-rift Stage 2, Iberia was an independent plate. Beginning in the late Santonian, however, its northern margin evolved into an active margin, initiating the Pyrenean orogeny. Subsequent Iberia-Eurasia convergence drove contraction along the Tethyan margin of the Iberian Plate, and intraplate stresses transmitted into cratonic Iberia ultimately produced the Paleogene–Miocene inversion of the Iberian Basin and the formation of the Iberian and Catalan Coastal chains.

Late Jurassic-Early Cretaceous rift systems around Iberia

Several late Permian–Mesozoic basins are distributed around the Iberia-Eurasia plate boundary and the North Atlantic Iberian margin (Fig. 13). Late Jurassic to early Albian rifting is not recorded synchronously across the Iberia and Eurasia plates, as indicated by subsidence analyses from different basins. The reviewed basins (Fig, 13) display similar subsidence phases, which are slightly diachronous and tend to become younger from the western Jeanne d'Arc and Lusitanian basins toward the northeastern Iberian and Pyrenean rift systems (Asti *et al.*, 2022; Borel, 1997; Stampfli, 2000; Tavani *et al.*, 2018; Tugend *et al.*, 2015).

Most of these basins underwent two syn-rift cycles, the first during the Late Jurassic–Berriasian pp., and the second during the Barremian–Albian pp. (Fig. 13) These two cycles are separated by a Neocomian event (Berriasian pp.–Hauterivian) of reduced subsidence, characterized by significant uplift and erosion within the Iberian rift system, particularly in the Maestrat and Garraf basins (Salas and Casas, 1993; Salas *et al.*, 2001). This Neocomian phase of reduced subsidence was also recorded in several other basins (Fig. 13), including the Basque-Cantabrian and Aquitaine basins (Stampfli, 2000), the Parentis Basin (Brunet, 1991), the Arzacq and Tarbes basins (Brunet, 1984), and the Bujaraloz oil exploration well, located on the SW margin of the present-day Cenozoic Ebro Basin (Vargas *et al.*, 2009).

Cenozoic contractional inversion

As a result of the Iberia-Eurasia convergence since the late Cretaceous, a contractional tectonic regime was established in the present-day Iberian Chain, leding to the inversion of the Mesozoic Iberian Rift System and the development of a complex thrust system (Álvaro *et al.*, 1979; Guimerà, 2018; Guimerà *et al.*, 2004; Liesa *et al.*, 2018; Salas *et al.*, 2001). A crustal thickening resulted from this contraction (Gómez-Ortiz *et al.*, 2005; Guimerà *et al.*, 2016; Rey Moral *et al.*, 2003), and extensive areas of the chain were uplifted to elevations above 1000m (Casas-Sainz and Cortés Gracia, 2002; Casas-Sainz and de Vicente, 2009; Guimerà and González, 1998; Vergés and Fernández, 2006).

In this context, the Maestrat and Garraf basins experienced a mild inversion of the major Mesozoic normal faults that bounded them (Penyagolosa, Xert, Herbers and Montmell faults), whereas most of the contraction was located in the Linking Zone, a newly formed fold-and-thrust system north of the Xert and Herbers faults (Guimerà, 1983, 1984, 2018; Nebot and Guimerà, 2016a, b; Salas *et al.*, 2001). A total contraction of 18.4km was estimated from the structural cross-sections across the Maestrat Basin.

CONCLUSIONS

Since the late Permian, and concurrently with the opening of the Alpine Tethys, the North Atlantic, and the Bay of Biscay domains, three main rifting phases developed across Iberia and its oceanic margins: (i) late Permian–Middle Triassic, (ii) Late Jurassic, and (iii) Barremian–early Albian. These phases were separated by post-rift periods or events of relative tectonic quiescence.

The Maestrat and Garraf basins formed through these rifting phases involving extensional systems that affected the uppermost crust, with basal faults reaching depths of 7 to 10km. These basins are most distinctly defined during the Barremian–early Albian phase, whereas the sedimentary records from earlier phases are more widespread.

The Hettangian rifting event firstly recognized in eastern Iberia in this work may be associated with the onset of rift systems in the Central Atlantic-Alpine domain and the opening of the Neotethys following the Carnian. This period corresponds to the final closure of the Paleotethys in the Mediterranean and Middle East regions.

During the late Permian–Middle Triassic rifting phase, high-angle normal faults oriented NW–SE to WNW–ESE, along with additional N–S-trending faults, created a structural framework of horsts, grabens, and semigrabens. These structures involved the Variscan basement and overlying successions, including the upper Permian, Triassic Buntsandstein, Lower Muschelkalk, and the lower part of the Middle Muschelkalk These units exhibit thicker successions on the hanging walls of the extensional faults, including growth strata. In contrast, the remaining Triassic units show no significant variations in thickness. The Upper Muschelkalk, however, is interpreted as a syn-rift unit, as evidenced by the subsidence curves presented in this study and those reported in the literature for the Triassic Iberian Basin. The syn-rift nature of the Upper Muschelkalk is also evidenced in the correlation of petroleum wells of the Maestrat Basin, where a post-Buntsandstein high-angle normal fault oriented NNE-SSW controlled the Middle Triassic as syn-rift and the Keuper as post-rift. From the Upper Triassic Keuper facies to the Oxfordian, the results suggest that sedimentation took place during a post-rift phase.

Rifting during the Late Jurassic is less well defined, as its structures are largely obscured by younger overlying rocks. However, faults from this period have been identified in the northern part of the Maestrat Basin, where they have since been reactivated as thrusts. Furthermore, both north and south of the Maestrat Basin, uppermost Jurassic rocks lie unconformably over Lower Jurassic and Triassic units, respectively. Following the Late Jurassic Rifting Cycle 2, the reduction or cessation of subsidence throughout the Neocomian has been interpreted as an interval marked by relative tectonic quiescence and decelerating subsidence between the Late Jurassic and the Barremian–early Albian rift cycles

The Maestrat and Garraf basins are best defined during the Barremian–early Albian rifting phase. The Maestrat Basin is bounded by two major faults: the E–W-trending Herbers Fault to the north and the NW–SE-trending Penyagolosa Fault to the southwest. Additional E–W-trending faults within this region divide La Salzedella, Morella, and Galve sub-basins. In the latest Aptian (Benassal Formation), the Orpesa Sub-basin developed, bounded to the northwest by the NE–SW-trending Benicàssim Fault. The Garraf Basin is bounded by NE-SW faults, being their downthrown hanging wall located to the SE, and their displacement increasing in this direction. Hence subsidence is increasing from El Montmell to Sitges sub-basins.

During the late Eocene to Early Miocene tectonic inversion of the Maestrat and Garraf basins, several normal faults were reactivated as thrusts, and new thrust faults also formed. In the northern part of the Maestrat Basin, the Linking Zone fold-and-thrust belt developed just north of the Herbers Fault, which experienced only minor inversion. In the southwest, the central segment of the Penyagolosa Fault was inverted by several kilometers, with the amount of inversion decreasing towards the northwest and southeast. These contractional structures were strongly influenced by the earlier Mesozoic extensional framework. The total contraction is estimated at 18.4km in a NNE–SSW direction. The faults bounding the Garraf Basin were only slightly inverted during the Cenozoic contraction. Instead, new thrusts formed northwest of the basin, uplifting it and exposing it to erosion.

ACKNOWLEDGEMENTS

We are grateful to Jesús García-Senz, an anonymous reviewer, and the invited editor Josep Anton Moreno-Bedmar for their suggestions and corrections, which helped to improve the manuscript. Financial support by the Grup de Recerca Reconegut per la Generalitat de Catalunya 2021 SGR-Cat 00349 "Geologia Sedimentària", and the I+D+i research projects IBERCAFO (PID2024-159218NB-I00), SABREM (PID2020-117598GB-I00), and IBERINSULA (PID2020-113912GB-I00), funded by the MCIN/AEI/10.13039/501100011033 and the European Regional Development Fund (ERDF), is appreciated.

REFERENCES

Albrich, S., Bernaus, J.M., Boix, C., Caus, E., Martín-Closas, C., Salas, R., Vicedo, V., Villalonga, R., 2006. Caracterización bioestratigráfica y paleoambiental del Cretácico inferior (Berriasiense-Barremiense) del Macizo de Garraf (Cadena Costera Catalana). Revista Española de Micropaleontología, 38, 429-452.

Allen, P.A., Allen, J.R., 1990. Basin analysis: principles and applications. Oxford, Blackwell Scientific Publications, 451 pp.

Alonso, A., Floquet, M., Mas, R., Melédez, A., 1993. Late Cretaceous Carbonate Platforms: Origin and Evolution. Iberian Range. Spain. In: Sim, T., Scott, R.W., Masse, J.P. (eds.). Cretaceous Carbonate Platforms. American Association of Petroleum Geologists, Memoir 56, 297-316.

Alvaro, M., Capote, R., Vegas, R., 1979. Un modelo de evolución geotectónica para la cadena Celtibérica. Acta Geológica Hispánica, 14, 172-181.

Anadón, P., Colombo, F., Esteban, M., Marzo, M., Robles, S., Santanach, P., Solé Sugrañes, L. 1979. Evolución tectonoestratigráfica de los Catalánides. Acta Geológica Hispánica, Homenatge a Lluís Solé i Sabarís, 14, 242-270.

Arche, A., López-Gómez, J., 1996. Origin of the Permian-Triassic Iberian Basin, central eastern Spain. Tectonophysics, 266, 443-464.

Arche, A., López-Gómez, J., Marzo, M., Vargas, H., 2004. The siliciclastic Permian-Triassic deposits in Central and Northeastern Iberian Peninsula (Iberian, Ebro and Catalan Basin): A proposal for correlation. Geologica Acta, 2, 305-320.

Arthaud, F., Matte, P., 1977. Late Paleozoic strike-slip faulting in southern Europe and northern Africa: Result of a right-Lateral shear zone between Appalachians and the Urals. Geological Society of America Bulletin, 88, 1305-1320.

Asti, R., Saspiturry, N., Angrand, P., 2022. The Mesozoic Iberia-Eurasia diffuse plate boundary: A wide domain of distributed transtensional deformation progressively focusing along the North Pyrenean Zone. Earth-Science Reviews, 230, 104040.

Aurell, M., Bádenas, B., Casas, A.M., Salas, R., 2009. Peritidal Carbonate–Evaporite Sedimentation Coeval to Normal Fault Segmentation During the Triassic–Jurassic Transition, Iberian

Chain. In: Jarvis, I., Nichols, G., Williams, E., Paola, C. (eds.). Sedimentary Processes, Environments and Basins. Wiley-Blackwell, 223-246. DOI: 10.1002/9781444304411.ch10.

Aurell, M., 1990. El Jurásico superior en la Cordillera Ibérica Central (provincias de Zaragoza y Teruel). Análisis de cuenca. Ph.D. Thesis, Universidad de Zaragoza, 389pp.

Aurell, M., 1991. Identification of systems tracts in low-angle carbonate ramps: examples from the Upper Jurassic of the Iberian Chain (Spain). Sedimentary Geology, 73, 101-115.

Aurell, M., Bádenas, B., Gasca, J.M., Canudo, J.I., Liesa, C.L., Soria, A.R., Moreno-Azanza, M., Najes, L., 2016. Stratigraphy and evolution of the Galve sub-basin (Spain) in the Middle Tithonian-Early Barremian: Implications for the setting and age of some dinosaur fossil sites. Cretaceous Research, 65, 138-162.

Aurell, M., Meléndez, A., San Roman, J., Guimerà, J., Roca, E., Salas, R., Alonso, A., Mas, R., 1992. Tectónica sinsedimentaria distensiva en el límite Triásico-Jurásico en la Cordillera Ibérica. Salamanca, III Congreso Geológico de España y VIII Congreso Latinoamericano de Geologia. Actas, 1, 50-54.

Aurell, M., Meléndez, G., Olóriz, F., Bádenas, B., Caracuel, J.E., García-Ramos, J.C., Goy, A., Linares, A., Quesada, S., Robles, S., Rodríguez-Tovar, F.J., Rosales, I., Sandoval, J., Suárez de Centi, C., Tavera, J.M., Valenzuela, M., 2002. Jurassic. In: Gibbons, W., Moreno, T. (eds.). The Geology of Spain. London, Geological Society, 213-254.

Aurell, M., Soria, A.R., Bádenas, B., Liesa, C.L., Canudo, J.I., Gasca, J.M., Moreno-Azanza, M., Medrano-Aguado, E., Meléndez, A., 2018. Evolution of a Barremian synrift sequence in continental to coastal environments with a widespread presence of vertebrate remains (Blesa Formation, Oliete sub-basin, Spain). Journal of Iberian Geology, 44(2), 285-308.

Aurell, M., Torromé, D., Gasca, J.M., Calvín, P., Pérez-Pueyo, M., Parrilla-Bel, J., Medrano-Aguado, E., Martín-Closas, C., Vicente, A., Sierra-Campos, P., Canudo, J.I., 2022. Latest Cretaceous palaeogeographic evolution of northeast Iberia: Insights from the Campanian continental Montalbán subbasin (Spain). Earth-Science Reviews, 235, 104251.

Baqués, V., Travé, A., Roca, E., Marín, M., Cantarero, I., 2012. Geofluid behaviour in successive extensional and compressional events: a case study from the southwestern end of the Vallès-Penedès Fault (Catalan Coastal Ranges, NE Spain). Petroleum Geoscience, 18, 17-31.

Bond, G., Kominz, M.A., 1984. Construction of tectonic subsidence curves for the Early Paleozoic miogeocline, southern Canadian Rocky Mountains: implications for subsidence mechanisms, age of break up and crustal thinning. Geological Geological Society of America Bulletin, 95, 155-173.

Bover-Arnal, T., Salas, R., Moreno-Bedmar, J.A., Bitzer, K., 2009. Sequence stratigraphy and architecture of a Late Early-Middle Aptian carbonate platform succession from the western Maestrat Basin (Iberian Chain, Spain). Sedimentary Geology, 219, 280-301.

Bover-Arnal, T., Moreno-Bedmar, J.A., Salas, R., Skelton, P.W., Bitzer, K., Gili, E., 2010. Sedimentary evolution of an Aptian syn-rift carbonate system (Maestrat Basin, E Spain): effects of accommodation and environmental change. Geologica Acta, 8, 249-280.

Bover-Arnal, T., Salas, R., Guimerà, J., Moreno-Bedmar, J.A., 2014. Deep incision on an Aptian carbonate succession indicates major sea-level fall in the Cretaceous. Sedimentology, 61, 1558-1593.

Bover-Arnal, T., Pascual-Cebrian, E., Skelton, P.W., Gili, E., Salas, R., 2015. Patterns in the distribution of Aptian rudists and corals within a sequence-stratigraphic framework (Maestrat Basin, E Spain). Sedimentary Geology, 321, 86-104.

Bover-Arnal, T., Moreno-Bedmar, J.A., Frijia, G., Pascual-Cebrian, E., Salas, R., 2016. Chronostratigraphy of the Barremian–Early Albian of the Maestrat Basin (E Iberian Peninsula): integrating strontium-isotope stratigraphy and ammonoid biostratigraphy. Newsletters on Stratigraphy, 49(1), 41-68.

Bover-Arnal, T., Salas, R., Guimerà, J., Moreno-Bedmar, J.A., 2022. Eustasy in the Aptian world: A vision from the eastern margin of the Iberian Plate. Global and Planetary Change, 214, 103849.

Bover-Arnal, T., Guimerà, J., Moreno-Bedmar, J.A., Ferràndez-Cañadell, C., Salas, R., 2024. Aptian major changes in accommodation. New sedimentary evidence from the Maestrat Basin (E Iberia). Sedimentary Geology, 459, 106546.

Bover-Arnal, T., Pascual-Cebrian, R., Moreno-Bedmar, J.A., Salas, R., 2025. Strontium-isotope stratigraphy of the Aptian–Albian transition in the western Maestrat Basin (E Iberia). Geologica Acta, 23(27), 1-21.

Borel, G.D., 1997. Dynamique de l'extension mésozoique du domaine briançonnais: les Préalpes médianes au Lias. Ph.D. Thesis, Université de Lausanne, 157pp.

Brunet, M.F., 1984. Subsidence history of the Aquitaine Basin determined from subsidence curves. Geological Magazine, 121, 421-428.

Brunet, M.F., 1991. Subsidence et géodynamique du bassin d'Aquitaine. Relations avec l'ouverture de l'Atlantique. Ph.D. Thesis, Université Paris Curie, Mémoire Sciences de la Terre, 91-8, 288pp.

Bulard, P.F., 1972. Le Jurassique moyen et supérieur de la Chaine Ibérique sur la bordure du Basin de l'Ebre (Espagne). Ph.D. Thesis, Univ. Nice, 702pp.

Caja Rodríguez, M.A., 2004. Procedencia y diagénesis de los sedimentos del Jurásico Superior-Cretácico Inferior (facies Weald) en las subcuencas occidentales de la cuenca del Maestrazgo, cordillera Ibérica oriental. Ph.D. Thesis, Universidad Complutense de Madrid, 305pp.

Caja, M.A., Marfil, R., Lago, M., Salas, R., Permanyer, A., 2007. Provenance discrimination of Lower Cretaceous syn-rift sandstones (eastern Iberian Chain, Spain): Constraints from detrital modes, heavy minerals, and geochemistry. In: Arribas, J., Critelli, S., Johnsson, M.J. (eds.). Sedimentary Provenance and Petrogenesis: Perspectives from Petrography and Geochemistry. Geological Society of America Special Paper, 420, 181-197.

Calvet, F., Tucker, M.E., Henton, J.M., 1990. Middle Triassic carbonate ramp systems in the Catalan Basin, northeast Spain: facies, systems tracts, sequences and controls. In: Tucker, M.E., Wilson, J.L., Crevello, P.D., Sarg, J.R., Read, J.F. (eds.). Carbonate Platforms. Facies, Sequences and Evolution. Special Publication of the International Association of Sedimentologists, 9, 79-108.

Campos, S., Aurell, M., Casas, A., 1996. Origen de las brechas de la base del Jurásico en Morata de Jalón (Zaragoza). Geogaceta, 20(4), 887-889.

Campos-Soto, S., Cobos, A., Caus, E., Benito, M.I., Fernández-Labrador, L., Suarez-Gonzalez, P., Quijada, I.E., Mas, R., Royo-Torres, R., Alcalá, L., 2017. Jurassic Coastal Park: A great diversity of palaeoenvironments for the dinosaurs of the Villar del Arzobispo Formation (Teruel, eastern Spain). Palaeogeography, Palaeoclimatology, Palaeoecology, 485, 154-177.

Canérot, J., 1974. Recherches géologiques aux confins des chaînes ibérique et catalane (Espagne). Ph.D. Thesis, Université Paul Sabatier, 517pp.

Canérot, J., 1991. Comparative study of the Eastern Iberides (Spain) and the Western Pyrenees (France) Mesozoic basins. Palaeogeography, Palaeoclimatology, Palaeoecology, 87, 1-28.

Canérot, J., Cugny, P., Pardo, G., Salas, R., Villena, J., 1982. Ibérica Central-Maestrazgo. In: García, A. (ed.). El Cretácico de España. Madrid, Universidad Complutense, 273-344.

Capote, R., 1983. La fracturación subsecuente a la orogenia Hercínica. In: Libro Jubilar José María Ríos. Madrid, Ministerio de Industria, 2, 17-25.

Casas-Sainz, A.-M., Cortés Gracia, A.L., 2002. Cenozoic landscape development within the Central Iberian Chain, Spain. Geomorphology, 44(1-2), 19-46.

Casas-Sainz, A.-M., de Vicente, G., 2009. On the tectonic origin of Iberian topography. Tectonophysics, 474(1-2), 214-235.

Cohen, K., Harper, D., Gibbard, P., Car, N., 2025. The ICS international chronostratigraphic chart this decade. Episodes, 48(1), 105-115.

Coromines, J., 1997. Perímetre de protecció per a les captacions municipals d'aigua potable de la comarca del Garraf. Estudis i monografies, núm 19. Diputació de Barcelona, Servei del Medi Ambient, 101pp.

Esteban, M. Julià, R., 1973. Discordancias erosivas intrajurásicas en los Catalánides. Acta Geológica Hispánica, 8, 153-157.

Esteban, M., Robles, S., 1979. Período preorogénico, el Mesozoico. Acta Geológica Hispánica, 11(3), 73-78.

Esteban, M., 1973. Petrología de las calizas cretácicas del sector central de los Catalánides (prov. de Tarragona y Barcelona). Ph.D. Thesis, Universitat de Barcelona, 425pp.

Etheve, N., Mohn, G., Frizon de Lamotte, D., Roca, E., Tugend, J., Gómez□Romeu, J., 2018. Extreme Mesozoic crustal thinning in the eastern Iberia margin: The example of the Columbrets Basin (Valencia Trough). Tectonics, 37(2), 636-662.

Fang, P., Tugend, J., Mohn, G., Kusznir, N., Ding, W., 2021. Evidence for rapid large-amplitude vertical motions in the Valencia trough (Western Mediterranean) generated by 3D subduction slab roll-back. Earth and Planetary Science Letters, 575, 117179.

Fernández, S.R., 1985. El Bajociense en la Cordillera Ibérica. Ph.D. Thesis Universidad Complutense, Madrid, 850pp.

Floquet, M., Alonso, A., Meléndez, A., 1982. Cretácico superior, Cameros-Castilla. In: García, A. (ed.). El Cretácico de España. Madrid, Universidad Complutense, 387-456.

Gale, A.S., Mutterlose, J., Batenburg, S., Gradstein, F.M., Agterberg, F.P., Ogg J.G., Petrizzo, M.R., 2020. The Cretaceous Period. In: Gradstein, F.M., Ogg, J.G., Schmitz, M.D., Ogg, G.M. (eds.). Geologic Time Scale. Elsevier, 1023-1086.

García, A., Mas, R., Segura, M., Carenas, B., García-Hidalgo, J.F., Gil, J., Alonso, A., Aurell, M., Bádenas, B., Benito, M.I., Meléndez, A., Salas, R., 2004. Segunda fase de post-rifting: Cretácico Superior. In: Vera, J.A. (ed.). Geología de España. Madrid, Sociedad Geológica de España–Instituto Geológico y Minero de España, 510-522.

Garcia, R., Moreno-Bedmar, J.A., Bover-Arnal, T., Company, M., Salas, R., Latil, J.L., Martín-Martín, J.D., Gomez-Rivas, E., Bulot, L.G., Delanoy, G., Martínez, R., Grauges, A., 2014. Lower Cretaceous (Hauterivian-Albian) ammonite biostratigraphy in the Maestrat Basin (E Spain). Journal of Iberian Geology, 40, 99-112.

García-Mondejar, J., 1989. Strike-Slip Subsidence of the Basque -Cantabrian Basin of Northern Spain and its Relationship to Aptian-Albian Opening of Bay of Biscay. In: Tankard, A.J., Balkwill, H.R. (eds.). Extensional Tectonics and Stratigraphy of the North Atlantic Margins. Memoir American Association of Petroleum Geologists, 46, 395-409.

García-Penas, Á., Aurell, M., Zamora, S., 2024. Sedimentary evolution and distribution of benthic fauna of an Aptian protected bay (Oliete Subbasin, Spain). Sedimentary Geology, 461, 106577.

Gawthorpe, R.L., Leeder, M.R., 2000. Tectono-sedimentary evolution of active extensional basins. Basin Research, 12(3-4), 195-218.

Giner, J., 1980. Estudio sedimentológico y diagenético de las formaciones carbonatadas del Jurásico de los Catalánides, Maestrazgo y Rama Aragonesa de la Cordillera Ibérica (sector oriental). Ph.D. Thesis, Universitat de Barcelona, 315pp.

Gómez, J.J., 1979. El Jurásico en facies carbonatadas del sector levantino de la Cordillera ibérica. Ph.D. Thesis, Universidad Complutense, Madrid. Seminarios de Estratigrafía. Serie Monográfica, 4, 687pp.

Gómez, J.J., Goy, A., 2004. Jurásico inferior. In: Vera, J.A. (ed.). Geología de España. Madrid, Sociedad Geológica de España–Instituto Geológico y Minero de España, 495-500.

González, A., Guimerà, J., Luzón, A., 1998. Edad Oligoceno superior-Mioceno inferior para las superficies de erosión conservadas en el flanco SW de la cubeta de Bordón (Província de Teruel, España). Geogaceta, 24, 155-158.

Gómez-Ortiz, D., Tejero-López, R., Babín-Vich, R., Rivas-Ponce, A., 2005. Crustal density structure in the Spanish Central System derived from gravity data analysis (Central Spain). Tectonophysics 403 (2005) 131-149.

Goy, A., Gómez, J.J., Yébenes, A., 1976. El Jurásico de la Rama castellana de la Cordillera Ibérica (mitad Norte). I. Unidades litoestratigráficas. Estudios geológicos, 32, 391-423.

Guimerà J., 1988. Estudi estructural de l'enllaç entre la serralada Ibérica i la serralada costanera Catalana. Ph.D. Thesis, Universitat de Barcelona, 600pp.

Guimerà, J., 1983. Évolution de la deformation alpine dans le NE de la Chaîne Ibérique et dans la Chaîne Côtière Catalane. Comptes-rendus de l'Académie des sciences, Paris, Série 2, 297(5), 425-430.

Guimerà, J., 1984. Palaeogene evolution of deformation in the northeastern Iberian Peninsula. Geological Magazine, 121(5), 413-420.

Guimerà, J., 1994. Cenozoic evolution of eastern Iberia: Structural data and dynamic model. Acta Geológica Hispánica, 29(1), 57-66.

Guimerà, J., 2004. Cadenas con cobertera: Las Cadenas Ibérica y Costera Catalana. In: Vera, J.A. (ed.). Geología de España. Madrid, Sociedad Geológica de España–Instituto Geológico y Minero de España, 602-607.

Guimerà, J., 2018. Structure of an intraplate fold-and-thrust belt: The Iberian Chain. A synthesis. Geologica Acta, 16(4), 427-438.

Guimerà, J., Álvaro, M., 1990. Structure et évolution de la compression alpine dans la Chaîne Ibérique et la Chaîne côtière catalane (Espagne). Bulletin de la Société Géologique de France, 6(2), 339-348.

Guimerà, J., Salas, R., 1996. Inversión terciaria de la falla normal mesozoica que limitaba la subcuenca de Galve (Cuenca del Maestrazgo). Geogaceta, 20(7), 1701-1703.

Guimerà, J., González, A., 1998. El relieve de la Cadena Ibérica como un producto de la compresión alpina. Geogaceta, 24, 163-166.

Guimerà, J., González, A., Salas, R., Sancho, C., 2010. Origin and preservation of the Late contractional relief of an intraplate thrust-belt: the NE Iberian Chain (Iberian Peninsula). Geophysical Research Abstracts, 12. EGU2010-5137.

Guimerà, J., Rivero, L., Salas, R., Casas, A., 2016. Moho depth inferred from gravity and topography in an intraplate area (Iberian Chain). Tectonophysics, 666, 134-143.

Haq, B.H., Handerbol, J., Vail, P.R., 1987. Chronology of fluctuating sea levels since the Triassic. Science, 235,1156-1167.

Haq, B.U., Hardenbol, J., Vail, P.R., 1988. Mesozoic and Cenozoic chronostratigraphy and cycles of sea-level change. Society of Economic Paleontologists and Mineralogists, 42, 71-108.

Humphrey, E., Gomez-Rivas, E., Martín-Martín, J.D., Neilson, J., Salas, R., Guimerà, J., 2022. Depositional and structural controls on a fault-related dolostone formation (Maestrat Basin, E Spain). Basin Research, 34, 961-990.

Kooi, H., Burrus, J., Cloetingh, S., 1992. Lithospheric necking and regional isostasy at extensional basins: part 1, Subsidence and gravity modeling with an application to the Gulf of Lions margin (SE France). Journal of Geophysical Research, 97, 17553-17571.

Lanaja, J.M., 1987. Contribución de la exploración petrolífera al conocimiento de la Geología de España. Madrid, Instituto Geológico y Minero de España, Servicio de Publicaciones del Ministerio de Industria y Energía 465pp.

Le Vot, M., Biteau, J.J., Masset, J.M., 1996. The Aquitaine basin: oil and gas production in the foreland of the Pyrenean fold-and-thrust belt. New exploration perspectives. In: Ziegler, P.A., Horvàth, F. (eds.). Peri-Tethys Memoir 2: Structure and Prospects of Alpine Basins and Forelands. Mémoires du Muséum National d'Histoire Naturelle, 170, 159-171.

Liesa, C. L., Soria, A. R., Meléndez, N., Meléndez, A., 2006. Extensional fault control on the sedimentation patterns in a continental rift basin: El Castellar Formation, Galve sub-basin, Spain. Journal of the Geological Society, 163, 487-498.

Liesa, C.L., Casas, A.M., Simóm, J.L., 2018. La tectónica de inversión en una región intraplaca: la Cordillera Ibérica. Revista de la Sociedad Geológica de España 31(2), 23-50.

López Gómez, J., Arche Miralles, A., 1992. Las unidades litoestratigráficas del Pérmico y el Triásico inferior y medio en el sector SE de la Cordillera Ibérica. Estudios geológicos, 48, 123-143.

Madarieta-Txurruka, A., Pedrera, A., Galindo-Zaldívar, J., Estrada, F., García-Senz, J., Ercilla, G., 2025. Mode of Continental Thinning and Breakup Along the North Iberian-Armorican Conjugate Margins in the Bay of Biscay. Journal of geophysical Research: Solid Earth, 10(10), e2025JB031754.

Marín Pérez, M.A., 2025. Influence of the Mesozoic structural inheritance on the fault reactivation in the central Catalan Coastal Ranges (Catalan Margin, NW Mediterranean). Paleogene and Neogene tectonostratigraphic evolution. Ph.D. Thesis, Universitat de Barcelona. 222pp. https://www.tesisenred.net/handle/10803/695041

Marín, M., Roca, E., Marcuello, A., Cabrera, L., Ferrer, O., 2021. Mesozoic structural inheritance in the Cenozoic evolution of the central Catalan Coastal Ranges (western Mediterranean): Structural and magnetotelluric analysis in the Gaià-Montmell High. Tectonophysics, 814, 228970. DOI: https://doi.org/10.1016/j.tecto.2021.228970

Marín, M., Carola, E., Beamud, E., Bover-Arnal, T., López-Clanco, M., Garcés, M., Roca, E., Costa, E., Ferrer, O., Cabrera, L., 2025. Paleogene kinematics of the central Catalan Coastal Ranges: temporal constraints from magneto-chronology and provenance analysis in synorogenic deposits in the SE margin of the Ebro Basin (NE Spain). Geologica Acta, 23(2), 1-25, I-XVI.

Martín-Chivelet, J., López-Gómez, J., Aguado, R., Arias, C., Arribas, J., Arribas, M.E., Aurell, M., Bádenas, B., Benito, M.I., Bover-Arnal, T., Casas-Sainz, A., Castro, J.M., Coruña, F., de Gea, G.A., Fornós, J.J., Fregenal-Martínez, M., García-Senz, J., Garófano, D., Gelabert, B., Giménez, J., González-Acebrón, J., Guimerà, J., Liesa, C.L., Mas, R., Meléndez, N., Molina, J.M., Muñoz, J.A., Navarrete, R., Nebot, M., Nieto, L.M., Omodeo-Salé, S., Pedrera, A., Peropadre, C., Quijada, I.E., Quijano, M.L., Reolid, M., Robador, A., Rodríguez-López, J.P., Rodríguez-Perea, A., Rosales, I., Ruiz-Ortiz, P.A., Sàbat, F., Salas, R., Soria, A.R., Suarez-Gonzalez, P., Vilas, L., 2019. The Late Jurassic–Early Cretaceous Rifting. In: Quesada, C., Oliveira, J.T. (eds.). The Geology of Iberia: A Geodynamic Approach. Volume 3: The Alpine Cycle. Heidelberg, Springer, 60-63. DOI: https://doi.org/10.1007/978-3-030-11295-0.

Martín-Closas, C., Vicente, A., Pérez-Cano, J., Sanjuan, J., Bover-Arnal, T., 2017. On the Earliest occurrence of Tolypella section Tolypella in the fossil record and the age of major clades in extant Characeae. Botany Letters, 165, 23-33.

Martín-Closas, C., Albalat, D., Colombo, F., Vilà, M., Vicente, A., Ossó, À., Vicedo, V., Bover-Arnal, T., 2025. A refugium for charophytes during the maximum post-Palaeozoic sea-level highstand in the Turonian of Tarragona (Catalonia, Spain). Geologica Acta, 23(11), 1-19.

Martínez, R.M., Lago, M., Valenzuela, J.I., Vaquer, R., Salas, R., Dumitrescu, R., 1997. El volcanismo triásico y jurásico del sector SE de la Cadena Ibérica y su relación con los estadios de rift mesozoicos. Boletín Geológico y Minero, 108(4), 367-376.

Martínez-Abad, J.L., 1991. Cuenca del Maestrazgo. Correlación de sondeos I-I'. In: López, F. (coord.). Estudio geológico del Maestrazgo y de la mitad meridional de los Catalánides. INYPSA-IGME, unpublished.

Martín-Martín, J. D., Gómez-Rivas, E., Bover-Arnal, T., Travé, A., Salas, R., Moreno-Bedmar, J.A., Tomás, S., Corbella, M., Teixell, A., Vergés, J., Stafford, S.I., 2013. The Upper Aptian to Lower Albian syn-rift carbonate succession of the southern Maestrat Basin (Spain): Facies architecture and fault-controlled stratabound dolostones. Cretaceous Research, 41, 217-236.

Martín-Martín, J.D., Sanfeliu, T., Gómez-Gras, D., 2005. Mineralogía de arcillas cerámicas. El permo-trias de Castelló. Publicacions de la Universitat Jaume I, Col•lecció Atena, 13, 280pp.

Mas, J.R., Alonso, Á., Guimerà, J., 1993. Evolución tectonosedimentaria de una cuenca extensional intraplaca: La cuenca finijurásica-eocretácica de Los Cameros (La Rioja-Soria). Revista de la Sociedad Geológica de España, 6, 129-144.

Mas, R., García, A., Salas, R., Meléndez, A., Alonso, A., Aurell, M., Bádenas, B., Benito, M.I., Carenas, B., García-Hidalgo, J.F., Gil, J., Segura, M., 2004. Segunda fase de rifting: Jurásico Superior-Cretácico Inferior. In: Vera, J.A. (ed.). Geología de España. Madrid, Sociedad Geológica de España–Instituto Geológico y Minero de España, 503-510.

Mckenzie, D., 1978. Some remarks on the development of sedimentary basins. Earth and Planetary Science Letters, 40, 25-32.

Mercedes-Martín, R., Arenas, C., Salas, R., 2014a. Diversity and factors controlling widespread occurrence of syn-rift Ladinian microbialites in the western Tethys (Triassic Catalan Basin, NE Spain). Sedimentary Geology, 313, 68-90.

Mercedes-Martín, R., Salas, R., Arenas, C., 2014b. Microbial-dominated carbonate platforms during the Ladinian rifting: sequence stratigraphy and evolution of accommodation in a fault-controlled setting (Catalan Coastal Ranges, NE Spain). Basin Research, 26(2), 269-296.

Miall, A.D., 2010. The geology of stratigraphic sequences. Springer Science & Business Media, 522pp.

Moreno-Bedmar, J.A., Albalat, D., Mallofré, A., Ossó, A., Vilà, M., 2016. Estratigrafia mesozoica i nous cefalòpodes de l'Aptià del Vendrell, sud-oest del massís del Garraf (Catalunya). Nemus, 6, 61-72.

Moreno-Bedmar, J.A., Bulot, L., Latil, J.L., Martínez, R., Ferrer, O., Bover-Arnal, T., Salas, R., 2008. Precisiones sobre la edad de la base de la Fm. Escucha, mediante ammonoideos, en la subcuenca de la Salzedella, Cuenca del Maestrat (E Cordillera Ibérica). Geo-Temas, 10, 1269-1272.

Moreno-Bedmar, J.A., Robert, E., Matamales-Andreu, R., Bover-Arnal, T., 2017. Review of the Early Albian ammonites of the Montmell Formation near Marmellar (Salou-Garraf Basin, Tarragona, Catalonia, Spain). Carnets de Géologie, 17(1), 1-10.

Navarrete, R., Rodríguez-López, J.P., Liesa, C.L., Soria, A.R., Mesquita, F., Veloso, L., 2013. Changing physiography of rift basins as a control on the evolution of mixed siliciclastic–carbonate back-barrier systems (Barremian Iberian Basin, Spain). Sedimentary Geology, 289, 40-61.

Nebot, M., 2016. Mesozoic extension and Cenozoic contraction in the Eastern Iberian Chain (Maestrat Basin). Ph.D. Thesis. Universitat de Barcelona, 110pp. http://www.tdx.cat/bitstream/10803/403983/1/MNM_PhD_THESIS.pdf

Nebot, M., Guimerà, J., 2016a. Structure of an inverted basin from subsurface and field data: the Late Jurassic-Early Cretaceous Maestrat basin (Iberian Chain). Geologica Acta, 14(2), 155-177.

Nebot, M., Guimerà, J., 2016b. Kinematic evolution of a fold-and-thrust belt developed during basin inversion: the Mesozoic Maestrat basin, E Iberian Chain. Geological Magazine, 155(3), 630-640.

Nebot, M., Guimerà, J., 2016c. La extensión Triásica en el substrato de la Cuenca del Maestrat, y evidencias de tectónica salina en las evaporitas en facies Muschelkalk medio (Cadena Ibérica Oriental). Geo-Temas, 16(1), 241-244.

Nebot, M., Guimerà, J., 2016d. Inversión cenozoica de la Cuenca mesozoica del Maestrat: evolución cinemática del cinturón de pliegues y cabalgamientos desarrollado en su margen norte (Cadena Ibérica oriental). Geo-Temas, 16 (2), 527-530.

Nirrengarten, M., Manatschal, G., Tugend, J., Kusznir, N.J., Sauter, D., 2018. Kinematic Evolution of the Southern North Atlantic: implications for the Formation of Hyperextended Rift Systems. Tectonics, 37, 89-118. DOI: https://DOI: doi.org/10.1002/ 2017TC004495.

Ortí, F., Pérez-López, A., Salvany, J.M., 2017. Triassic evaporites of Iberia: Sedimentological and palaeogeographical implications for the western Neotethys evolution during the Middle Triassic-Earliest Jurassic. Palaeogeography, Palaeoclimatology, Palaeoecology, 471, 157-180.

Ortí-Cabo, F., 1982-83. Sur les conditions de dépot, la diagenese et la structure des évaporites triasiques dans l'est de l'Espagne. Sciencies de la Terre, XXV(2), 179-199.

Pedrera, A., Ruiz-Constán, A., García-Senz, J., Azor, A., Marín-Lechado, C., Ayala, C., Díaz de Neira, J.A., Rodríguez-Fernández, L.R., 2020. Evolution of the south-Iberian paleomargin: From hyperextension to continental subduction. Journal of Structural Geology, 138, 104122.

Pedrera, A., García-Senz, J., Peropadre, C., Robador, A., López-Mir, B., Díaz-Alvarado, J., Rodríguez-Fernández, L.R., 2021. The Getxo crustal-scale cross-section: testing tectonic models in the Bay of Biscay-Pyrenean rift system. Earth-Science Reviews, 212, 103429.

Permanyer, A., 1990. Sedimentologia i diagènesi dels esculls miocènics de la Conca del Penedès. Barcelona, Institut d'Estudis Catalans, 320pp.

Permanyer, A., Salas, R., 2005. Integrated thermal model, diagenetic history and oil correlation in western Mediterranean, Spain. In: IV ALAGO Workshop on Basin Modelling, Buenos Aires, 4pp.

Pimentel, N., Pena dos Reis, R., 2016. Petroleum systems of the west Iberian margin: a review of the Lusitanian Basin and the deep offshore Peniche Basin. Journal of Petroleum Geology, 39(3), 305-326.

Querol, X., Salas, R., Pardo, G., Ardévol, L., 1992. Albian coal-bearing deposits of the Iberian Range in northeastern Spain. In: McCabe, J.P., Parrish, J.T. (eds.). Controls and distribution and quality of Cretaceous Coals. Boulder, Colorado. Geological Socyety of America, Special Paper, 267, 193-208.

Ramos, A., Pedrera, A., García-Senz, J., López-Mir, B., Salas, R., 2023. Seismic evidence for ductile necking of the mid-lower crust beneath the Columbrets Basin (Western Mediterranean). Terra Nova, 35(5), 404-412.

Rey Moral, C., Gómez Ortiz, D., Tejero López, R., 2003. Geometría del Moho en el Centro Peninsular obtenida a partir de datos gravimétricos. Boletín Geológico y Minero, 114(1), 41-56

Roca, E., 1996. La cubeta mesozoica de las Columbrets: aportaciones al conocimiento de la estructura del surco de Valencia. Geogaceta, 20(7), 1711-171.

Roca, E., Guimerà, J., 1992. The Neogene structure of the eastern Iberian margin: structural constraints on the crustal evolution of the Valencia trough (western Mediterranean). In: Banda, E., Santanach, P. (eds.). Geology and Geophysics of the Valencia trough, Western Mediterranean. Tectonophysics, 203, 203-218.

Roca, E., Guimerà, J., Salas, R., 1994. Mesozoic extensional tectonics in the southeast Iberian Chain. Geological Magazine, 131(2), 155-168.

Roma, M., Ferrer, O., Roca, E., Pla, O., Escosa, F.O., Butillé, M., 2018. Formation and inversion of salt-detached ramp-syncline basins. Results from analog modeling and application to the Columbrets Basin (Western Mediterranean). Tectonophysics, 745, 214-228.

Rossi, C., Goldstein, R.H., Marfil, R., Salas, R., Benito, M.I., Permanyer, A., de la Peña, J.A., Caja, M.A., 2001. Diagenetic and oil migration history of the Kimmeridgian Ascla formation, Maestrat basin, Spain. Marine and Petroleum Geology, 18(3), 287-306.

Salas, R., 1987. El Malm i el Cretaci Inferior entre el Massís de Garraf i la Serra d'Espadà. Anàlisi de conca. Ph.D. Thesis, Universitat de Barcelona, 541pp. https://www.tesisenred.net/handle/10803/669675

Salas, R., Casas, A., 1992. Historia de la subsidencia, anomalías gravimétricas y evolución mesozoica de las cuencas del margen oriental de Iberia. In: III Congreso Geológico de España y VIII Congreso Latinoamericano de Geología. Salamanca, Actas, 2, 112-116.

Salas, R., Casas, A., 1993. Mesozoic extensional tectonics, stratigraphy, and crustal evolution during the Alpine cycle of the eastern Iberian basin. Tectonophysics, 228, 33-55.

Salas, R., Guimerà, J., 1996. Main structural features of the Lower Cretaceous Maestrat basin (Eastern Iberian Range). Geogaceta, 20(7), 1704-1706.

Salas, R., Permanyer, A., 2003. Evidencias de generación de hidrocarburos en la formación de margas del Mas d'Ascla (Jurásico superior, Cadena Ibérica oriental) y su relación con el campo de Amposta de la Cuenca de Tarragona. Boletín Geológico y Minero, 114(1), 75-86.

Salas, R., Alonso, A., Aurell, M., Carbó, A., Casas. A., Gómez, J.C., Guimerà, J., Martín-Closas, C., Mas, R., Meléndez, A., Meléndez, G., Meléndez, N., Rivero, L., Serra-Kiel, J., 1992. Sequence stratigraphy and subsidence analysis of the Jurassic and Cretaceous in the Iberian basin (Iberian Range) Spain. In: Sequence Stratigraphy of European Basins, CNRS-IFP Dijon, France. Abstracts volume, 211.

Salas, R., Martín-Closas, C., Querol, X., Guimerà, J., Roca, E., 1995. Evolución tectonosedimentaria de las cuencas del Maestrazgo y Aliaga-Penyagolosa durante el Cretácico inferior. In: Salas, R., Martín-Closas, C. (eds.). El Cretácico inferior del Nordeste de Iberia. Barcelona, Publicacions de la Universitat de Barcelona 13-94.

Salas, R., Guimerà, J., Mas, R., Martín-Closas, C., Menéndez, A., Alonso, A., 2001. Evolution of the Mesozoic Central Iberian Rift System and its Cainozoic inversion (Iberian Chain). In: Ziegler, P.A., Cavazza, W., Roberston, A.H.F., Crasquin-Soleau, S. (eds.). Peri-Tethys Memoir 6: Peri-Tethyan Rift/Wrench Basins and Passive Margins, Memoires du Museum National d'Histoire Naturelle, Paris, 186, 145-186.

Salas, R., García-Senz, J., Guimerà, J., Bover-Arnal, T., 2010. Opening of the Atlantic and development of the Iberian intraplate rift basins during the late Jurassic-early Cretaceous, In: Pena dos Reis, R., Pimentel, N. (eds.). II Central & North Atlantic Conjugate Margins Conference, Lisboa, 245-248.

San Román, J., Aurell, M., 1992. Palaeogeographical significance of the Triassic-Jurassic unconformity in the north Iberian basin (Sierra del Moncayo, Spain). Palaeogeography, Palaeoclimatology, Palaeoecology, 99(1-2), 101-117.

Sánchez-Moya, Y., Arribas, J., Gómez-Gras, D., Marzo, M., Pérez-Arlucea, M., Sopeña, A., 2004a. Inicio del rifting. El comienzo del relleno continental. In: Vera, J.A. (ed.). Geología de España. Madrid, Sociedad Geológica de España–Instituto Geológico y Minero de España, 485-487.

Sánchez-Moya, Y., Arribas, J., García-Gil, S., Gómez-Gras, D., Marzo, M., Meléndez, M., Pérez-Arlucea, M., Sopeña, A., 2004b. Máxima expansión del rifting. Sucesiones continentales, marinas y evaporíticas. In: Vera, J.A. (ed.). Geología de España. Madrid, Sociedad Geológica de España–Instituto Geológico y Minero de España, 489-492.

Sclater, J.M., Christie, P.A.F., 1980. Continental stretching: an explanation of the post Mid-Cretaceous subsidence of the central North Sea basin. Journal of Geophysical Research, 85, 3711-3739.

Seillé, H., Salas, R., Pous, J., Guimerà, J., Gallart, J., Torné, M., Romero-Ruiz, I., Diaz, J., Carbonell., R., Mas, R., 2015. Crustal structure of an intraplate thrust belt: The Iberian Chain revealed by wide-angle seismic, magnetotelluric soundings and gravity data. Tectonophysics, 663, 339-353.

Sopeña, A., López-Gómez, J., Arche, A., Pérez-Arlucea, M., Ramos, A., Virgili, C., Hernando, S., 1988. Permian and Triassic rift basins of the Iberian peninsula. In: Manspeizer, W. (ed.). Triassic-Jurassic Rifting. Amsterdam, Elsevier, Development in Geotectonics, 22B, 757-786.

Stampfli, G.M., Kozur, H.W., 2006. Europe from the Variscan to the Alpine cycles. In: Gee, D.G., Stephenson, R.A. (eds.). European Litoshere Dynamics. London, The Geological Society, 32 (Memoirs), 57-82.

Stampfli, G.M., 2000. Tethyan oceans. In: Bozkurt, E., Winchester, J.A., Piper, J.D.A. (eds.). Tectonics and magmatism in Turkey and surrounding area. Geological Society of London, Special Publication, 173, 163-185.

Stampfli, G.M., Borel, G.D., Marchant, R., Mosar, J., 2002. Western Alps geological constraints on western Tethyan reconstructions. Journal of the Virtual Explorer, 8, 77-106.

Stapel, G., Cloetingh, S.A.P.L., Pronk, B., 1996. Quantitative subsidence analysis of the Mesozoic Evolution of the Lusitanian Basin (western Iberian margin). Tectonophysics, 266, 493-507.

Steckler, M.S., Watts, A.B., 1978. Subsidence of the Atlantic-type continental margin of New York. Earth and Planetary Science Letters, 41, 1-13.

Tavani, S., Bertok, C., Granado, P., Piana, F., Salas, R., Vigna, B., Muñoz, J. A., 2018. The Iberia-Eurasia plate boundary east of the Pyrenees. Earth-Science Reviews, 187, 314-337.

Tucker, M.E., Calvet, F., Hunt, D., 1993. Sequence stratigraphy of carbonate ramps: systems tracts, models and application to the Muschelkalk carbonate platforms of eastern Spain. Special Publications of the International Association of Sedimentologists 18, 397-415.

Tugend, J., Manatschal, G., Kusznir, N.J., 2015. Spatial and temporal evolution of hyperextended rift systems: Implication for the nature, kinematics, and timing of the Iberian-European plate boundary. Geology, 43(1), 15-18.

Van Wees, J.-D., Stephenson, R.A., 1995. Quantitative modelling of basin and rheological evolution of the Iberian Basin (Central Spain): implications for lithospheric dynamics of intraplate extension and inversion. Tectonophysics, 252, 163-178.

Van Wees, J.D., Arche, A., Beijdorf, C.G., López-Gómez, J., Cloethingh, S., 1998. Temporal and spatial variations in tectonic subsidence in the Iberian basin (eastern Spain): inferences from automated forward-modelling of high-resolution stratigraphy (Permian-Mesozoic). Tectonophysics, 300, 285-310.

Vargas, H., Gaspar-Escribano, J.M., López-Gómez, J., Van Wees, J.D., Cloetingh, S., De la Horra, R., Arche, A., 2009. A comparison of the Iberian and Ebro Basins during the Permian and Triassic, eastern Spain: a quantitative subsidence modelling approach. Tectonophysics, 474, 160-183.

Vegas, R., Banda, E., 1982. Tectonic framework and Alpine evolution of the Iberian Peninsula. Earth Evolution Sciences, 4, 320-343.

Vendeville, B.C., Jackson, M.P.A.,1992. The rise of diapirs during thin-skinned extension. Marine and Petroleum Geology, 9(4), 331-354.

Vennin, E., Aurell, M., 2001. Stratigraphie sequentielle de l'Aptien du sous-basin de Galvé (Province de Teruel, NE de l'Espagne). Bulletin de la Societe Geologique de France, 172, 397-410.

Vera, J.A., 2001. Evolution of the South Iberin Continental Margin. In: Ziegler, P.A., Cavazza, W., Robertson, A.H.F., Crasquin-Soleau, S. (eds.). Peri-Tethyan Rift/Wrench Basins and Passive Margins. Mémoires du Muséum National d'Histoire Naturelle, 186, 109-143.

Vera, J.A. (Ed.). (2004). Geología de España. Instituto Geológico y Minero de España, 884pp.

Vergés. J.; Fernàndez, M., 2006. Ranges and basins in the Iberian Peninsula: their contribution to the present topography. In: Gee, D. G. & Stephenson, R. A. (eds) 2006. European Lithosphere Dynamics. London, The Geological Society, 32 (Memoirs), 223–234.

Vergés, J., García-Senz, J., 2001. Mesozoic evolution and Cainozoic inversion of the Pyrenean Rift. In: Ziegler, P.A., Cavazza, W., Robertson, A.H.F. Crasquin-Soleau, S. (eds.). Peri-Tethyan Rift/Wrench Basins and Passive Margins. Mémoires du Muséum National d'Histoire Naturelle, 186, 187-212.

Viallard, P., 1973. Recherches sur le cycle alpin dans la chaîne Ibérique sud-occidentale. Ph.D. Thesis, Univ. Toulouse, 445pp.

Virgili, C., Sopena, A., Ramos, A. Arche, A., Hernando, S., 1983. El relleno posthercínico y el comienzo de la sedimentación Mesozoica. In: Libro Jubilar José María Ríos. Madrid, Ministerio de Industria, 2, 25-36.

Vissers, R.L.M., Meijer, P.T., 2012. Mesozoic rotation of Iberia: subduction in the Pyrenees? Earth-Science Reviews, 110(1-4), 93-110.

Watts, A.B., 1981. Atlantic continental margin: subsidence history, crustal structure and thermal evolution: Geology of Passive Continental Margins. In: History Structure and Sedimentologic Record (with special emphasis on the Atlantic margin). American Association of Petroleum Geologists, Education Course Note Series 19, Ch. 2.

Ziegler, P.A., 1988. Evolution of the Arctic-North Atlantic and the Western Tethys. Memoir American Association of Petroleum Geologists, 43, 198pp.

Manuscript received August 2025;
revision accepted April 2026;
published June 2026.